Journal Pre-proof

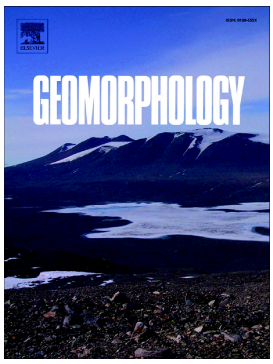


# Aged carbon mineralisation from headwater peatland floodplains in the Peak District, UK

D. MAlderson, M.G. Evans, M.H. Garnett, F. Worrall

PII: S0169-555X(24)00221-6

DOI: https://doi.org/10.1016/j.geomorph.2024.109271

Reference: GEOMOR 109271

To appear in: *Geomorphology*

Received date: 21 November 2023

Revised date: 23 May 2024

Accepted date: 23 May 2024

Please cite this article as: D. MAlderson, M.G. Evans, M.H. Garnett, et al., Aged carbon mineralisation from headwater peatland floodplains in the Peak District, UK, *Geomorphology* (2023), https://doi.org/10.1016/j.geomorph.2024.109271

# Aged carbon mineralisation from headwater peatland floodplains in the Peak District, UK

Alderson[1], D. M, Evans[1], M. G.,Garnett[2], M. H. and Worrall[3], F.

[1] Department of Geography, University of Manchester, Manchester, UK

[2] NEIF Radiocarbon Laboratory, SUERC, East Kilbride, Scotland, UK

[3]Department of Earth Sciences, Science Laboratories, University of Durham, Durham, UK

## Key words

Floodplain dynamics; Carbon cycling; aged organic carbon; radiocarbon dating

## Abstract

Floodplains are dynamic ecosystems that cycle carbon, which is both delivered from upstream catchment sources and produced in-situ. These systems are being increasingly recognised as key environments of carbon processing, with the capacity for substantial carbon storage, in addition to acting as hotspots of carbon mineralisation. The balance of storage versus mineralisation is dependent on a number of controls including landscape position and environmental conditions. This study focuses on three headwater floodplains downstream of a highly eroded blanket bog peatland in the Peak District, UK. Previous research has shown that aged organic carbon from peatland sources,

has been stored in floodplains in this area, and therefore, we aimed to understand whether allochthonous carbon was being mineralised in this context. We examined sediment cores and analysed the radiocarbon ($^{14}C$) content of soil-respired $CO_2$, using a partitioning approach to scrutinise the depth and age relations of respiration in the individual floodplains, and patterns of age distributions downstream. Aged organic carbon was released from the upper and mid floodplain sites ($^{14}C$ ages of 682 and 232 years BP, respectively), whereas only modern dates were recorded at the lower site. The geomorphic context and sedimentology supported these results, with the stratigraphy suggesting a dominance of allochthonous deposition at the upper sites, but primarily in-situ soil development at the lower site. There were no trends of radiocarbon age with depth in the individual floodplains, suggesting that floodplain sediments were well mixed and that aged organic matter was being processed both at the surface and at depth in the uppermost sites. An isotope mass balance mixing model indicated the dominance of two sources of $CO_2$; recently fixed C3 organic matter (< 10 years old) and $CO_2$ produced by methanogenesis. The results indicate that floodplains in a relatively narrow halo around eroding headwater peatlands, could be important sites of aged carbon turnover originally derived from upstream sources. Reworked carbon does not transfer passively through the system and experiences periods of deposition where it can be subject to microbial action. This is an important consideration in other environments where organic carbon has previously been 'locked up' (e.g., permafrost regions) but is now under the threat of release due to climate change.



## Introduction

The understanding of the fluvial system as a passive pipe transporting forms of carbon from land to ocean has evolved (Battin et al., 2009), so that it is now well-established that rivers play an important and dynamic role in the terrestrial carbon cycle, storing, processing and transforming organic carbon

(OC) (Cole et al., 2007; Aufdenkampe et al., 2011; Wohl et al., 2017). Carbon transformation takes place not just in the river, but also in the wider fluvial environment. Floodplains are dynamic sedimentary settings, which experience growth and incision. Their characteristics are controlled both by relative position on a river's longitudinal profile, and by other catchment characteristics, such as climatic regime and topography. Floodplains are carbon-rich ecosystems, which source carbon both from the river and through pedogenesis on stable floodplain surfaces. Erosion and deposition of floodplain sediments are intimately linked to their capacity for carbon sequestration or release (Zehetner et al., 2009).

Floodplains have conventionally been viewed as zones of carbon sequestration, where the organic carbon originates as a product of pedogenic development between periods of overbank sediment deposition (Turner et al.,, 2015). However, this is to ignore the role of allochthonous (external) inputs, as a consequence of organic sediment loads deposited overbank (particularly in catchments with highly organic soils). Overbank deposition of OC-rich sediments is not well quantified, but is expected to be substantial (Cole et al., 2007). Increasingly, floodplains are also being recognised for their ability to sequester allochthonous OC (e.g., Galy and Eglinton, 2011; Lininger et al., 2019; Torres et al., 2020).

The residence time and potential for degradation of OC in floodplains, is controlled by geomorphological functioning and environmental conditions (Hoffmann et al., 2013). In mature, stable floodplains, particulate OC (POC) residence times may be long, and these landforms are likely to be 'hot spots' of carbon transformation over longer timescales (Hoffmann et al.,, 2009), where slow-acting microbial processes have sufficient time for decomposition and mineralisation of floodplain organic matter (OM) (Goulsbra et al., 2016). Substantial amounts of carbon may also be stored as a consequence of pedogenesis in these contexts. In active, transient floodplains, where there is high river-floodplain connectivity and/or destructive processes dominate, hot-moments (McClain et al., 2003) and hotspots of carbon transformation can occur, as POC is mineralised under

sub-aerial conditions on the floodplain surface, or is remobilised into the stream system at either short timescales (subsequent large flood events) or longer timescales (channel migration), where it is further exposed to in-stream oxidative processes (Battin et al., 2008).

OC in floodplain soils may originate from multiple sources: recent OC (fresh vegetation, in—situ production i.e., bacteria and algae), aged OC (soil OC developed in-situ or from other upstream landforms in the catchment) and rock-derived (petrogenic) OC. Soil OC may be sourced from vegetation, microbes, mycorrhizae and fauna, and sedimentary rock contributions. The stored OC may therefore vary in age, constrained in part by the maximum age of the landform of origin (primary pedogenic OC cannot be older than the floodplain although older carbon may be inherited from allochthonous sources). Gaseous carbon flux at the surface of a floodplain, is likely to be strongly controlled by the respiration of relatively recently fixed carbon at the soil surface. Radiocarbon ($^{14}C$) ages of respired $CO_2$ can indicate mineralization of previously stored carbon, with ages older than the known age of floodplain sediments, being indicative of reworked allochthonous sources for that carbon.

Peatlands are major terrestrial stores of OC (Yu, 2012) and peat is a common soil type in mid- to high-latitude headwater catchments. In degrading peatlands, substantial off-site fluxes of OC are the norm, from locations as diverse as Southeast Asia (Evans et al., 2014) to the UK (Pawson et al., 2012). Where erosion occurs in peat-dominated catchments, this can represent major sources of carbon to fluvial systems (Pawson et al., 2012), and the age of POC/dissolved OC (DOC) exported downstream can be considerable, reflecting the long-term storage of carbon in peatlands (Evans et al., 2022). The fate of this exported carbon is a significant uncertainty for understanding the role of peatland erosion in the terrestrial carbon cycle. As carbon export is primarily through the fluvial system, the role of rivers and floodplains in carbon cycling in this context is particularly relevant.

The relocation of OC from a peatland to a floodplain environment is significant, as high water tables in intact peatlands inhibit decomposition and preserve OC. Between the erosion of OC at one landform at an upstream location, and the re-deposition at another further downstream, there is ample opportunity for fluvial processing to take place, now widely recognised as important in global carbon cycling budgets (e.g. Battin et al., 2009), and often resulting in rapid decomposition. Floodplains are commonly cited as stores of fluvial carbon (Hoffmann et al., 2009), as burial within highly saturated floodplains may lead to reduced rates of microbial decomposition, and the potential for stabilization through binding to mineral substrate. However, the fluctuating water tables and consequent redox conditions of many floodplain environments, will likely lead to higher rates of decomposition than that experienced by in situ peatland OC in waterlogged conditions (assuming intact peatland functioning).

Previous work within the Peak District, UK suggests that re-deposition could lead to the production of C cycling hotspots, with only 20% of POC deposited onto headwater floodplains being actively buried (Evans et al., 2013). Understanding the redistribution and preservation/decomposition of terrestrial OM in highly organic catchments, is therefore important in the context of closing the terrestrial carbon balance for these systems. If old carbon eroded from peatlands enters long-term storage in floodplain sediments, then the net climate forcing of the peatland erosion is reduced. Whereas, if floodplain carbon is rapidly turned over, then erosional losses from peatlands will contribute considerably to detrimental climate forcing.

This paper aims to develop our mechanistic understanding of floodplain carbon dynamics in eroded/eroding highly organic headwater catchments, and to directly address the question of whether allochthonous carbon is being processed in headwater floodplains in this context. We test three hypotheses:

1. *Floodplain $^{14}C$ turnover is derived from a mixture of old allochthonous and young autochthonous sources.*
2. Where floodplain carbon sources are derived from modern allochthonous material, or autochthonous carbon deposition, radiocarbon age will get younger towards the surface of the floodplain so that: *$^{14}C$ gaseous production isolated from the upper floodplain surface is younger.*
3. If allochthonous sources of old carbon associated with upstream erosion are substantial, then the *average age of $CO_2$ emissions from floodplains will become younger with distance downstream in a river catchment,* reflecting reduced downstream inputs of old carbon, due to deposition in upstream sediment stores/mineralisation upstream.

## Study site

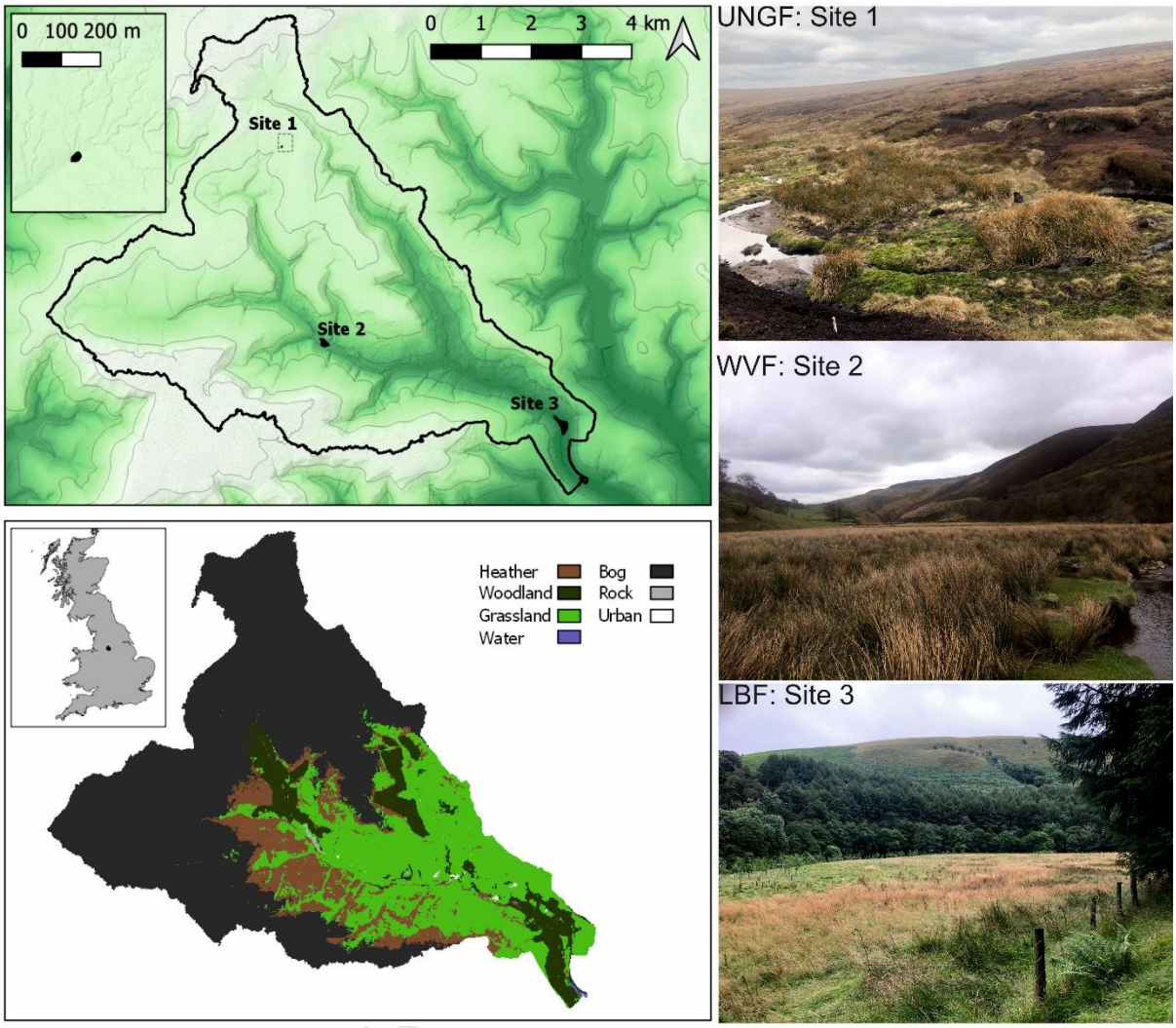


*Figure 1: Site locations in the Peak District, UK: headwater peatland catchment using a DEM of the Ashop and Alport catchments, dominant land use types in the catchments and site photos to demonstrate vegetation types. Site 1: Upper North Grain floodplain (UNGF), Site 2: Woodlands Valley Floodplain (WVF) and Site 3: Ladybower floodplain (LBF).*

The three hypotheses will be tested in the catchment of the River Ashop, which lies downstream of the severely eroding peatlands of the Peak District, UK, and which has previously been studied by Pawson et al., (2012) and Alderson et al., (2019a). The River Ashop catchment (approximately 50 $km^2$) in north-west England drains the slopes of the Bleaklow and Kinder Scout upland plateaux in the Peak District National Park, which support an extensive cover of eroded blanket peat (Figure 1). The River

Ashop, a single channel river (~10km) flows east, forming a confluence with the River Alport, before draining into Ladybower reservoir and forms the extreme headwaters of a much larger system linking the River Derwent and River Trent. The catchment elevation ranges from 631 m on Kinder Scout to 253 m at the catchment outlet. Annual discharge recorded at the catchment outflow (prior to the confluence with the River Alport) in 2006 ranged from 0.06-7.77 $m^3 s^{-1}$ (Pawson, 2008), while the TOC flux from the same research between 2005-2007 was 29.39 MgC $km^{-2} a^{-1}$ (Pawson et al., 2012). However, these discharge and TOC figures are not wholly representative, as they do not include the catchment area for the River Alport. Residence times in these steep headwater catchments are extremely short, in the order of hours (e.g. Stimson et al., 2017), and the export of particulate OC is episodic and event-driven (Hope et al., 1997), often during large storms.

The catchment geology is predominantly Carboniferous interbedded sandstones and mudstones (Millstone Grit series), which is characteristic of most of the Peak District (Wolverson-Cope, 1976). The soil types are deep peats on the plateau, stagnopodzols on the steep hillslopes and at lower elevations, brown earths. Blanket bog formation was a consequence of high elevations in these areas, and high rainfall and low temperatures (average annual precipitation 1313 mm and mean annual temperature 6.9°C: 2003-2013; Clay and Evans, 2017).

The vegetation type varies (Figure 1) with classic bog species on the peat, acidic grassland species on the valley slopes (with some conifer plantations and heather patches), and improved grassland in the lowland floodplains with wetland vegetation in close proximity to the river in some locations. Vegetation in the upper peat-dominated catchment includes species such as *Eriophorum vaginatum, Calluna vulgaris, Vaccinium myrtillus* and *Sphagnum* spp. In the lower catchment, the vegetation includes wetland rushes and grasses, with some moss in waterlogged areas including *Juncus effusus*, *Juncus articulatus*, *Festuca ovina*, *Nardus stricta*, *Deschampsia flexuosa*, *Polytrichum commune* and patches of *Sphagnum spp.*

The blanket peat has been subject to intense gully and surface erosion, due to pollution, climate changes and land use pressures over the past millennium (Evans et al., 2006). Bleaklow Plateau was amongst the most severely eroded peatlands in the UK (Evans and Lindsay, 2010). The land at present day is used for recreation, rough grazing and grouse moorland, and there have been substantial restoration works in the area to reduce POC loads, and restore water tables and native vegetation (Alderson et al., 2019b). High organic sediment flux from the catchment in the past, means that the floodplains have been potential sites of deposition, storage or turnover of allochthonous organic matter. The work of Pawson et al., (2012) has previously demonstrated conveyance losses of headwater carbon fluxes, and suggested that floodplains were a likely source of re-deposition and carbon turnover.

Further work by Alderson et al., (2019a), has shown that old carbon of peatland origin has been stored in floodplains downstream of the erosion. This research focused on a floodplain in the Woodlands Valley, where a case study floodplain was established as ~500 years old based on two wood $^{14}C$ dates and a suite of Infrared Stimulated Luminescence dates (Alderson et al., 2019a). Similarly, Alderson et al., (2019a) uses research from Evans and Lindsay (2010) to suggest that floodplain formation in this area was related to the onset of peat erosion, occurring at approximately 500 years BP. The $^{14}C$ age of organic inputs in a suite of cores (average: 3010 years BP excluding modern age; Alderson et al., 2019a) is consistent with significant inputs of allochthonous OM, and suggests that they formed in response to periods of intense erosion of the soils upstream during the last millennium. However, the question remains whether aged carbon is being turned over in this environment.

The study design was set up to examine the age of carbon being respired in floodplains along a downstream continuum in this upland headwater catchment (Figure 1). Three floodplains were selected along the Upper North Grain and River Ashop system, to examine the effect of an increasing number of prior depositional sites, on the reworking of allochthonous C. Site 1 (Upper North Grain

floodplain- UNGF: N 53° 26' 27.50" W -1° 50' 20.46") is within the peatland boundary of Bleaklow Plateau, and is the first substantial depositional site in the wider catchment and was studied by Evans et al., (2013). Site 2 (Woodlands Valley Floodplain- WVF- N 53° 24’ 20.7” W 001° 49’ 35.5”) is the first major floodplain in the catchment beyond the peatland limit (~5 km downstream of UNGF) and has also been the focus of prior research (Alderson et al., 2019a). Site 3 (Ladybower floodplain- LBF: N 53° 23’ 28.2” W 001° 45’ 14.1”) is approximately 8 km downstream of UNGF with considerable floodplain development upstream of the site, so that we would expect inputs of fluvial OC to be lower relative to in-situ fixation of carbon. Floodplains were selected on the basis of information garnered from previous research, access, and location above the reservoir, to avoid this additional consideration.

# Methods

## Experimental design to capture and assess $CO_2$ depth contributions,

A multidimensional research design was developed, including analysing sedimentary deposits, collecting and radiocarbon dating $CO_2$ respiration from the floodplain, and taking some limited gaseous carbon flux measurements for contextual purposes.

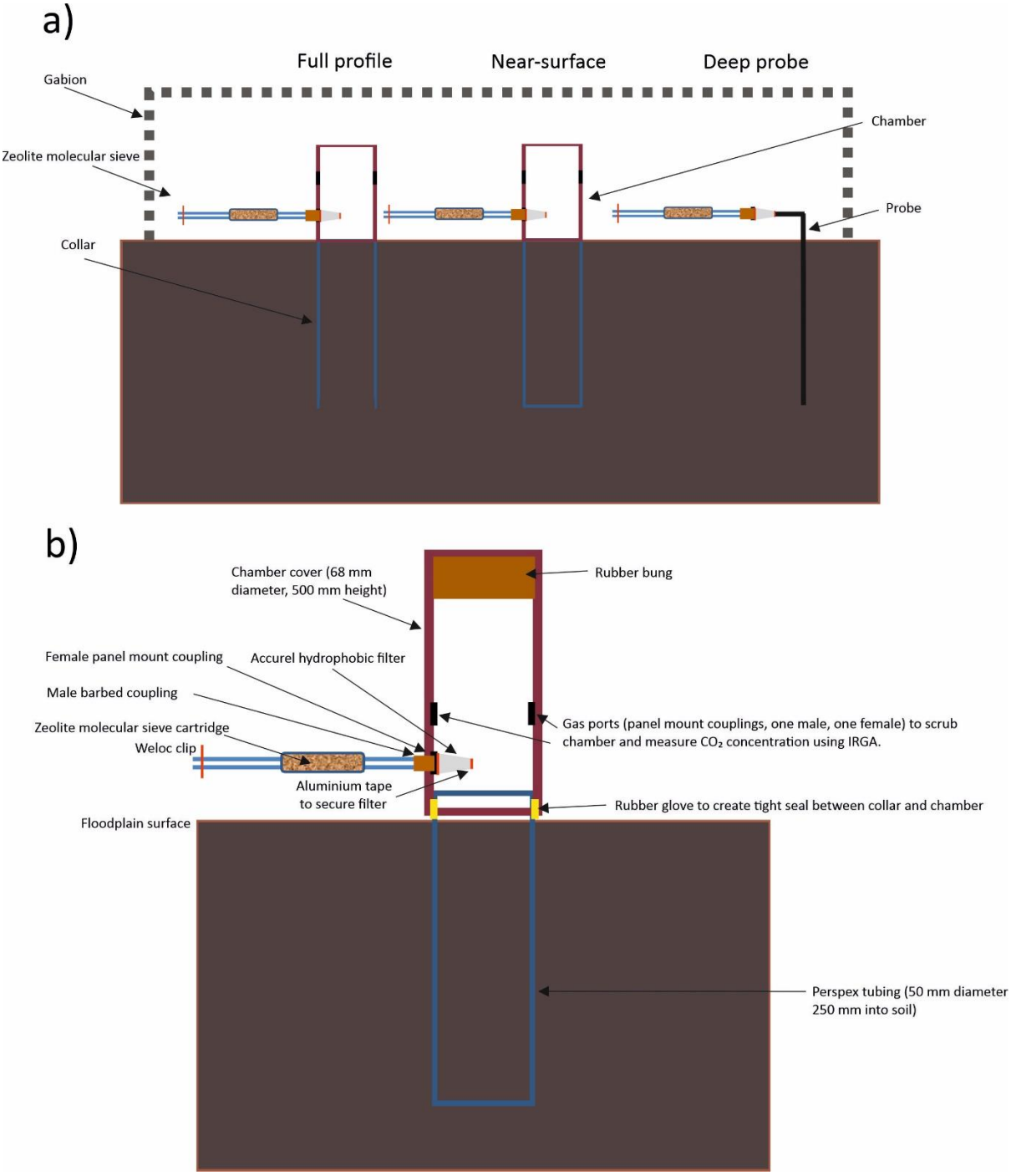


*Figure 2 a) Experimental set-up for $CO_2$ capture for radiocarbon dating. Full-profile, near-surface and deep probe plots. b) Detailed construction of chambers. Tubing was hammered into the ground to 250 mm for the full profile and near-surface plots, with the near-surface tubing removed, capped at the bottom and then re-inserted so that near-surface respiration was isolated. Respiration chambers were placed on top of the tubing 'collars' and the molecular sieve cartridges connected using auto-shut off couplings. The probe was placed into the soil with the bottom depth being 250 mm and connected to the molecular sieve using the same auto-shut off couplings.*

The experimental design for capturing gases emitted from the floodplains was based on Estop-Aragones et al., (2018), who partitioned deep and surface $^{14}CO_2$, to assess the impact of permafrost thaw on peatland carbon budgets. Our experiment contained two collar types and a probe to assess surface and deep $^{14}CO_2$ contributions to overall $CO_2$ collection (Figure 2a). In the near-surface collar, deep soil respiration is excluded from the $CO_2$ collection, as the collar is capped at the base (i.e. it is inserted, removed with the peat remaining in the middle, a cap put over the bottom and then the collar is re-inserted back into the hole made in the floodplain surface). Whereas in the full-profile collars, the $CO_2$ captured represents the whole soil profile, including from the soil beneath the collars as they are open-ended. The basal depth of the near-surface collar was 250 mm, and at this same depth, a probe was installed to collect $CO_2$ representative of deep peat respiration, which excludes respiration from the near-surface. There were three replicate plots of the experimental set up at each site.

Following Estop-Aragones et al., (2018) we used an isotope mass balance equation (Equation 1) to calculate the % of deep $CO_2$ contributing to floodplain surface $CO_2$ emissions.

Equation 1:

$$\text{Deep } CO_2(\%) = \left(\frac{FP^{14}CO_2 - NS^{14}CO_2}{Probe^{14}CO_2 - NS^{14}CO_2}\right)*100$$

For the purposes of this research, Deep $CO_2$ is the % contribution of $CO_2$ derived from the soil at or below 250 mm to the total respiration efflux, $FP^{14}CO_2$ is the $^{14}C$ content (in pMC; Stuiver and Polach, 1977) of the $CO_2$ collected from the full-profile collars, $NS^{14}CO_2$ is the $^{14}C$ content of the $CO_2$ collected from the near-surface collars, and $Probe^{14}CO_2$ is the $^{14}C$ content of the $CO_2$ collected from the soil, using the probes at the same depth as the base of the near-surface collars, which captures $CO_2$ from the pore spaces at this depth. Assuming that the soil characteristics allow gas to permeate up through the soil profile, these pore spaces should fill with respired $CO_2$ from 250mm and deeper. We expect that the $CO_2$ collected will be predominantly from the area surrounding the hydrophobic filter on the probe, particularly if the floodplain is saturated, as gas diffusion in water is low.

## Radiocarbon gas collection, dating and analysis

Perspex collars approximately 350 mm long (50 mm diameter) were installed into the ground surface using a mallet (Figure 2b). 100 mm of each collar remained aboveground to attach chambers for gas collection. The chambers were made from opaque black PVC and were 500 mm in length and 68 mm in diameter. A rubber seal was used to ensure a tight fit between the collar and chamber. Three holes were drilled into each chamber to attach auto-shutoff couplings; two to form a closed loop with a $CO_2$-measuring infrared gas analyser (IRGA; PP systems EGM-4, UK) and the third to attach a coupling to connect to a molecular sieve cartridge (MSC), for $CO_2$ capture. A gas permeable, hydrophobic filter (Accurel PP V8/2 HF, Membrana GmbH, Germany) was attached to the coupling on the inside of the chamber, to allow gas exchange, but prevent water incursion into the MSC. Rubber bungs were secured with waterproof tape to seal the top of the chambers.

The deep peat sampling probes were made of stainless-steel tube (6 mm outer diameter, 4 mm inner diameter, Swagelok) with a ca. 40 mm length of Isoversinic tubing (St Gobain, France) connected at the surface, with the same coupling as the respiration chambers (Garnett and Hardie, 2009). At the other end of the probe, an Accurel hydrophobic filter was used, to prevent water entering the probe when inserted into the peat, but allow gas exchange. The probe was directly attached to an MSC at the surface.

Zeolite molecular sieve cartridges (Garnett and Hartley, 2010) can efficiently capture $CO_2$ from respiring soil OM as they preferentially trap $CO_2$ over other gases such as $O_2$ and $N_2$. Detailed descriptions and diagrams of the design of the molecular sieves can be found in Hardie et al., (2005) and Garnett et al., (2009). The MSCs were constructed from borosilicate glass with a central chamber filled with Type 13X zeolite (Sigma-Aldrich, UK) for $CO_2$ absorption. Stainless steel wool was inserted into the tubing at each end of the narrower part of the tubing, to keep the sieve material in place. Isoversinic tubing was inserted at each end of the MSC and auto shut off couplings (Tom Parker Ltd,

UK and Colder Products Co., USA) attached for connection to the respiration chambers, as outlined above. These couplings automatically close when disconnected, thus preventing air from entering the sieve and contaminating the sample with atmospheric $CO_2$. WeLoc clips (Scandinavia Direct, UK) were also placed across the Isoversinic tubing to provide an additional seal when the MSC was not being used for sample collection. The MSCs were charged prior to sampling by heating, to 500°C for 0.5 hours and filled with high purity $N_2$ as in Garnett et al., (2019).

Collar installation took place between 21st-22nd August 2019. To prioritise dating of soil respiration, rather than aboveground plant respiration, vegetation was clipped 3 weeks prior to gas collection. However, the roots were not clipped or trenched, so root respiration cannot be completely excluded from calculations. The chambers were tested for leaks between 4th-5th September 2019, by checking the $CO_2$ build-up using the IRGA. Prior to $^{14}C$ sample collection, the chamber headspace was scrubbed to remove atmospheric $CO_2$, to as close to 0 ppm as possible(as a minimum <5 ppm), using a cartridge filled with soda lime and an IRGA (Hardie et al., 2005). The chambers were then left to start to accumulate $CO_2$ and then the molecular sieves were installed between the 11th-13th September 2019, allowing $CO_2$ collection via passive diffusion (Garnett and Hardie, 2009; Garnett et al., 2009).

Gabions (Fine Mesh Metals Ltd) were secured to the soil surface using stainless steel tent pegs, to protect the MSC from livestock interference. The concentrations were checked to make sure there was sufficient $CO_2$ in the respiration chambers after 17, 17 and 15 days respectively at UNGF, WVF and LBF, using an IRGA in a closed loop with the chamber (atmospheric $CO_2$ was removed from the IRGA using soda lime prior to connecting to the chambers). Repeat concentration measurements were also taken at UNGF after 27 days, because initial concentrations were lower than at other sites and were required to calculate how long the MSC should be left attached to the respiration chambers, to collect sufficient $CO_2$ for radiocarbon analysis. All molecular sieves were recovered on the 17th October 2019. Gas collection therefore lasted between 35-37 days with the exception of one

plot (WVF 3S) where the MSC was smashed by cattle after 23 days and a replacement attached for 11 days.

The molecular sieves were returned to the NEIF Radiocarbon Laboratory (East Kilbride, UK), where the sample $CO_2$ was recovered by heating (425 °C) and cryogenic collection (Garnett et al., 2019). After conversion to graphite, the samples were analysed for $^{14}C$ content at the Scottish Universities Environmental Research accelerator mass spectrometry Facility, with NIST Oxalic Acid II (National Institute of Standards and Technology, USA) used as the primary standard. An aliquot of the recovered $CO_2$ was used for determination of $\delta^{13}C$ (VPDB) using a Delta V isotope ratio mass spectrometer (Thermo-Fisher, Germany). Accuracy and precision of the isotope-ratio mass spectrometry was determined using international reference standards (IAEA-1, USGS-24 and IAEA-C5). Radiocarbon results were normalised to a $\delta^{13}C$ of -25 ‰ and expressed as radiocarbon years before present (BP; where 0 BP = AD 1950) and pMC (Stuiver and Polach, 1977) as is convention. Known $^{14}C$ age and background internal $CO_2$ reference gases (Air Products, UK) were trapped on molecular sieves, and processed alongside the samples, and provided $^{14}C$ and $^{14}C$ results within 1 σ of the consensus values.

In line with the experimental design, statistical analysis was designed as a factorial design with two fixed factors. The first factor was the difference between the monitoring sites, henceforward referred to as Site. The Site factor had 3 levels, one for each location on the transect (Figure 1). The second factor was the difference between the experimental types covered by the study with relation to sediment depth (henceforward referred to as Type), which were classified to give the factor three levels: full profile; near-surface and deep probe. The design was sufficient to estimate the significance of factors, as well as their interaction.

Prior to the ANOVA, outliers were identified using a Q-Q' plot. The application of the Levene test to the datasets showed that the assumption of homogeneous variance in ANOVA was reasonable. In addition, the Anderson-Darling test was used to check for normality (Anderson and Darling, 1952):

data were found to be normal at a probability of P > 0.9 rather than P > 0.95. The data were log-transformed and re-tested, but the probability of being normally-distributed was not changed by log-transformation. Therefore, to test the suitability of using ANOVA, ordinal logistic regression was applied as a non-parametric version of a two-way ANOVA; if the results were the same between the two approaches then it was considered reasonable to continue with a two-way ANOVA. The generalised $\eta^2$ approach (Vacha-Haase and Thompson, 2004) was used to calculate the magnitude of effects. Values from the ANOVA are presented as least-square means (otherwise known as marginal means). To evaluate differences between the levels of factors and interactions, values that were found to be significant, were post hoc tested using the Tukey test. Unless otherwise stated, significance refers to being significantly different from zero at the 95% probability ($p > 0.95$).

As a test of the experimental design, power analysis was applied to calculate the probability of type II error, given the levels of the Site and Type factors, with the effect sizes calculated and probability of type I error ($\alpha = 0.05$).

All analysis was performed using R v 4.3.1 in Rstudio with the following libraries – nortest, sjstats, effectsize, performance, marginaleffects, MASS and pwr2.

## Core collection and analysis

At WVF and LBF, cores were collected in circular Perspex tubes using a Van Walt Stitz corer on the same dates as the collars were installed. At UNGF, cores were collected using a standard Russian corer, with two drives taken to account for the full floodplain depth where possible. Multiple cores were collected at each site (see supplementary information) and scanned for optical imagery, X-radiography and micro-XRF using a Cox Analytical Systems Itrax core scanner with a step size of 200 microns for the entirety of each core. The XRF scans were completed using a molybdenum X-ray tube set at 60 kV and 50mA for the WVF and LBF cores, and 55 kV and 30mA for the peat-based UNGF cores. The count time for all cores was 15 seconds, which produces good excitation for a large range

of elements of interest in geochemistry. Cores were covered with a 6 µm film to prevent desiccation while scanning and to avoid contamination of the XRF detector.

Q-spec software from Cox analytical systems was used after scanning, to adjust the instrument settings, such as the X-ray tube and detector parameters, to enhance the mathematical model used to calculate the peak area for the XRF data. The enhanced mathematical model then re-evaluates each spectra using an automated batch procedure. This processing ultimately reduces the root mean square error of each spectra. The itraxR package in R (Bishop, 2021) was then used to clean the data further by only selecting spectra with a count rate per second between 15,000 and 45,000, and to deselect spectra where the RMSE was greater than 2.5. The itraxR package was further utilised to compile the optical imagery, radiographic imagery and selected XRF plots, to create diagrams where all the information collected from the core scanner can be visualised easily. The cores with the most complete stratigraphies were chosen for inclusion here, but all cores had similar elemental profiles and structures, with no major discrepancies noted.

## Respiration fluxes

Efflux data were collected using three separate methods during the same autumn campaign as gas collection for radiocarbon dating. Firstly, respiration flux measurements were taken from the full profile and short profile experimental plots at all three sites across two days (05/09/2019: WVF and LBF; 11/09/2019: UNGF), prior to molecular sieve attachment. Secondly, $CO_2$ fluxes were also taken from three replicate gas collars (150 mm diameter), that were hammered into the floodplain surface at each site to approximately 300 mm. These were taken on the 23/10/2019 and 28/10/2019 at all three sites, and additionally on 31/10/2019 at UNGF and WVF. These fluxes were taken using an EGM-4 IRGA. Thirdly, $CO_2$ and $CH_4$ fluxes were also measured at WVF only, on 03/10/2019 from two collars using a Los Gatos Research Ultra-Portable Greenhouse Gas Analyser (UGGA). Further details are outlined below.

Efflux data were collected using the IRGA attached to either the PVC respiration chambers on the full-profile and near-surface experimental plots, or a CPY-4 gas assimilation chamber on the separate collars at each site. For the latter, the chamber was flushed in the air between measurements. Only dark measurements (the respiration flux) were taken in the experimental plots as vegetation was clipped, and the chambers were opaque preventing photosynthesis. For the latter collars, light and dark measurements were taken so that NEE (Net Ecosystem Exchange) could be calculated if desired. As NEE is so dependent on light and temperature fluctuations (Lloyd and Taylor, 1994) which can vary over short timescales, because of environmental conditions such as cloud cover, only respiration fluxes are reported here. Measurements were taken across the three replicate plots designed for radiocarbon gas collection in both cases.

Further efflux data were collected only at the Woodlands Valley site on 3rd October 2019, using a UGGA, connected to an Eosense eosMX Chamber Multiplexer and two Eosense eosAC Soil Flux Chambers. Both chambers had a Decagon MAS-1 soil moisture probe attached and the first chamber also had a Decagon RT-1 soil temperature probe. The cycle time was approximately 10 minutes and 18 cycles were completed during the day (9 at each plot). The recorded air pressure was 1020 mbar. Only dark measurements were taken, because the chambers were opaque. The data were cleaned to remove noise at the beginning and end of the cycle where the chamber lid attaches/detaches to the gas collar, resulting in subsequent air influx into the chamber and photosynthesis able to take place. After data cleaning, the first 120 seconds of data were taken to compare to the results from data collection from the IRGA. Over the 10 minute period, $CO_2$ flux showed a strong linear trend (in all 18 cycles $R^2 = 0.99$, $P < 0.001$).

To transform the $CO_2$ respiration data from both the IRGA and UGGA into a gC/h equivalent, we used the method from Goulsbra et al., (2016) using Equation 2:

Equation 2: $$R = bv\left(\frac{44.01}{22.41 \times 1000}\right)\left(\frac{12}{44}\right)$$

where R is the efflux rate (gC/h); b is dC/dT as the change in the concentration of $CO_2$ in ppm/h (to find b, multiple linear regression is applied to the concentration readings over 120 second intervals, using the forecast function in Microsoft Excel and used to model the $CO_2$ flux over an hour, e.g. the difference between time 0 and time 120 multiplied by 30), v is the system volume in $m^3$ (either the CPY-4 chamber or pipe chambers attached to the full profile and short profile experimental plots plus the gas collars), $\left(\frac{44.01}{22.41 \times 1000}\right)$ is a unit conversion factor to convert from a concentration (i.e. ppm by volume in micromol/mol) to a mass equivalent of $CO_2$ (g), as one kg mol of gas (44.01 kg of $CO_2$) at STP occupies 22.41 $m^3$ ; the final term $\left(\frac{12}{44}\right)$ is used to convert $gCO_2$ to gC.

For Dc/Dt, where there were erroneous measurements, particularly at the beginning of the time period, time zero was modified to represent the beginning of the linear trend. Replicate measurements and replicate plots (three), were averaged to produce single respiration fluxes. Errors were appropriately propagated from replicate plots and measurements. For small fluxes i.e. where the change in ppm between time zero and time 120 seconds is small, caution must be taken in interpreting the results as the well known drift that takes place on IRGA instruments could have a substantial effect.

# Results

## Radiocarbon analyses

Table 1 provides results for the $CO_2$ captured by the MSCs for radiocarbon analysis. The volume of $CO_2$ collected by the MSCs ranged between 4.87-111.79 ml and trapping rates (accounting for days of exposure) varied between 0.13-3.02 ml $day^{-1}$. The plots that collected the most $CO_2$ were the probes at UNGF, with an average of 2.16 ml $day^{-1}$, followed by the surface profile (0.49 ml $day^{-1}$) and full profile plots (0.22 ml $day^{-1}$). This trend was not replicated at the other sites, as at WVF the highest $CO_2$ trap rate was at the surface profile (1.00 ml $day^{-1}$), and at LBF it was the full-profile plot (0.89 ml day$^{-}$

[1]). At both of these sites, the probes had the lowest trapping rates of 0.57 and 0.43 ml $day^{-1}$ respectively.

Fick's law (Bertoni et al., 2004), can be used to estimate an environment's $CO_2$ concentration from the rate of gas trapping in a diffusion sampler, since capture rate of $CO_2$ should be proportional to the environmental $CO_2$ concentration:

Equation 3: $$Ci = (Qi \times L)/(S \times t \times Di)$$

where Ci is the $CO_2$ concentration of the environment being sampled (inside the chamber), Qi represents the amount of $CO_2$ trapped during time t (duration of sampling), L and S are the length and cross-sectional area of the tube through which the $CO_2$ travels (i.e. from inlet to zeolite molecular sieve), and Di is the diffusion coefficient of $CO_2$ in air.

The Fick's law calculated $CO_2$ concentrations for chamber samples, are plotted against the IRGA-measured $CO_2$ values in Figure 3. There is a very strong correlation ($R^2 = 0.82$, $P < 0.001$) between the measured and estimated $CO_2$ concentrations, with Fick's law estimated concentrations being slightly (ca. 5 %) greater than measured values. This strong agreement between the time averaged measure (Fick's Law), and the point measurements of $CO_2$ flux, supports the notion that the $CO_2$ trapping rate did not vary substantially over time, and provides confidence that the $^{14}C$ results represent time averaged representations of the age of organic matter being mineralised in the floodplain system.

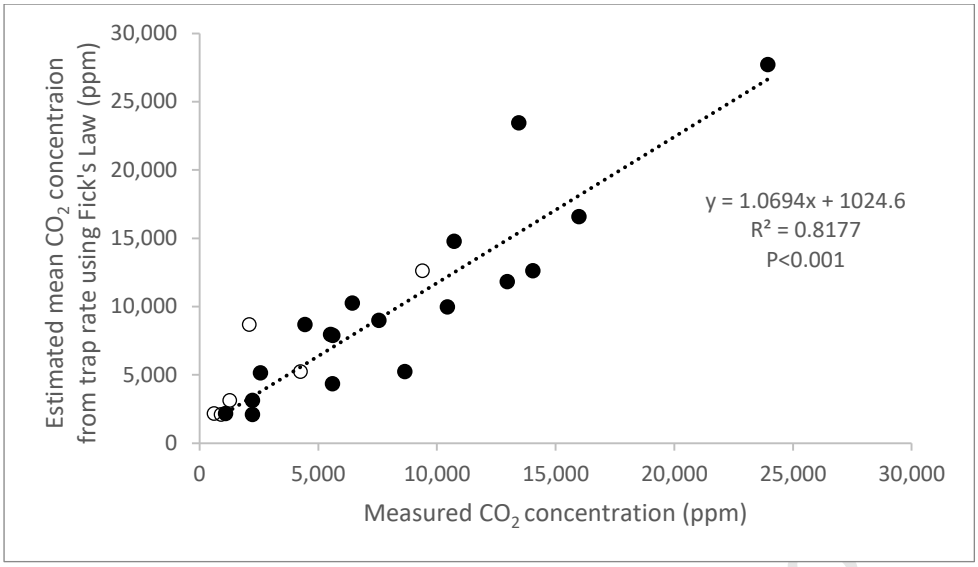


*Figure 3: Correlation between Fick's law estimates of average $CO_2$ concentration during sampling period and IRGA measured values. Measured concentrations taken after the start of sampling: Black: UNGF- 27 days, WVF- 17 days and LBF 15 days. Hollow: UNGF- 17 day (not included in the linear regression).*

*Table 1: Sample identifier: UNGF; WVF; LBF are the floodplain sites, 1; 2; 3 are the replicate plot numbers and P; NS; F are the probe, near-surface profile or full profile experiments respectively. During passive trapping isotopic fractionation occurs which affects the $\delta^{13}C$ measurement (but does not affect the $^{14}C$ result). The fractionation has been quantified as 4 ‰ (Garnett et al., 2009) and both uncorrected and corrected results are shown. See equation 1 for fraction calculations. All UNGF and WVF sites collected gas over 37 days with the exception of WVF 3S where collection took place over 11 days. Gas collection at LBF took place over 35 days. Graphs of $CO_2$ volume and trapping rates are provided in supplementary information.*

| Publication Code | Sample Identifier | $CO_2$ volume STP (ml) | Trapping rate (ml $day^{-1}$) | $^{14}C$ content (pMC) | pMC 1 σ error | Radiocarbon Age (years BP) | Radiocarbon Age 1 σ uncertainty | *$\delta^{13}C$-VPDB‰ | *$\delta^{13}C$-VPDB‰ + 4‰ | Fraction deep | Fraction shallow |
|---|---|---|---|---|---|---|---|---|---|---|---|
| SUERC-91240 | X243 UNGF 1P | 111.79 | 3.02 | 90.53 | 0.42 | 799 | 37 | -12.8 | -8.8 | N/A | N/A |
| SUERC-91241 | X300 UNGF 1NS | 20.20 | 0.55 | 87.34 | 0.41 | 1,088 | 37 | -28.8 | -24.8 | | |
| SUERC-91245 | X356 UNGF 1F | 7.27 | 0.20 | 96.08 | 0.44 | 321 | 37 | -24.2 | -20.2 | | |
| SUERC-91246 | X325 UNGF 2P | 63.69 | 1.72 | 90.97 | 0.42 | 760 | 37 | -14.6 | -10.6 | 0.03 | 0.97 |

| | | | | | | | | | | | |
|---|---|---|---|---|---|---|---|---|---|---|---|
| SUERC-91247 | X214 UNGF 2NS | 4.87 | 0.13 | 92.70 | 0.40 | 609 | 35 | -23.9 | -19.9 | | |
| SUERC-91248 | X217 UNGF 2F | 12.18 | 0.33 | 92.65 | 0.43 | 613 | 37 | -25.3 | -21.3 | | |
| SUERC-91249 | X256 UNGF 3P | 64.83 | 1.75 | 93.84 | 0.43 | 511 | 37 | -19.9 | -15.9 | 0.80 | 0.21 |
| SUERC-91250 | X263 UNGF 3NS | 29.36 | 0.79 | 89.61 | 0.41 | 882 | 37 | -20.8 | -16.8 | | |
| SUERC-91251 | X241 UNGF 3F | 5.00 | 0.14 | 92.97 | 0.43 | 585 | 37 | -23.9 | -19.9 | | |
| SUERC-91256 | X318 WVF 1P | 19.12 | 0.52 | 96.51 | 0.44 | 285 | 37 | -28.3 | -24.3 | N/A | N/A |
| SUERC-91257 | X249 WVF 1NS | 18.51 | 0.50 | 96.03 | 0.42 | 326 | 35 | -30.0 | -26.0 | | |
| SUERC-91258 | X328 WVF 1F | 38.56 | 1.04 | 97.30 | 0.45 | 220 | 37 | -31.8 | -27.8 | | |

| | | | | | | | | | | | |
|---|---|---|---|---|---|---|---|---|---|---|---|
| SUERC-91259 | X302 WVF 2P | 23.87 | 0.65 | 95.38 | 0.44 | 380 | 37 | -28.7 | -24.7 | N/A | N/A |
| SUERC-91260 | X210 WVF 2NS | 27.51 | 0.74 | 98.34 | 0.43 | 134 | 35 | -32.1 | -28.1 | | |
| SUERC-91261 | X262 WVF 2F | 23.84 | 0.64 | 98.78 | 0.46 | 99 | 37 | -35.4 | -31.4 | | |
| SUERC-91266 | X260 WVF 3P | 19.79 | 0.53 | 96.04 | 0.42 | 325 | 35 | -29.5 | -25.5 | N/A | N/A |
| SUERC-91267 | X248 WVF 3NS | 19.17 | 1.74 | 97.32 | 0.45 | 218 | 37 | -30.9 | -26.9 | | |
| SUERC-91268 | X316 WVF 3F | 11.95 | 0.32 | 98.65 | 0.45 | 109 | 37 | -31.0 | -27.0 | | |
| SUERC-91269 | X310 LBF 1P | 15.76 | 0.45 | 101.98 | 0.47 | n/a | n/a | -29.6 | -25.6 | N/A | N/A |
| SUERC-91270 | X309 LBF 1NS | 32.50 | 0.93 | 102.06 | 0.47 | n/a | n/a | -30.7 | -26.7 | | |

| | | | | | | | | | | | |
|---|---|---|---|---|---|---|---|---|---|---|---|
| SUERC-91271 | X341 LBF 1F | 21.91 | 0.63 | 102.57 | 0.47 | n/a | n/a | -30.6 | -26.6 | | |
| SUERC-91275 | X265 LBF 2P | 23.16 | 0.66 | 101.86 | 0.44 | n/a | n/a | -29.9 | -25.9 | N/A | N/A |
| SUERC-91276 | X238 LBF 2NS | 9.54 | 0.27 | 101.92 | 0.47 | n/a | n/a | -30.0 | -26.0 | | |
| SUERC-91277 | X233 LBF 2F | 51.60 | 1.47 | 102.16 | 0.47 | n/a | n/a | -30.1 | -26.1 | | |
| SUERC-91278 | X326 LBF 3P | 6.46 | 0.18 | 100.20 | 0.44 | n/a | n/a | -28.4 | -24.4 | 0.02 | 0.98 |
| SUERC-91279 | X250 LBF 3NS | 17.35 | 0.50 | 102.61 | 0.47 | n/a | n/a | -30.2 | -26.2 | | |
| SUERC-91280 | X253 LBF 3F | 19.78 | 0.57 | 102.57 | 0.45 | n/a | n/a | -30.4 | -26.4 | | |

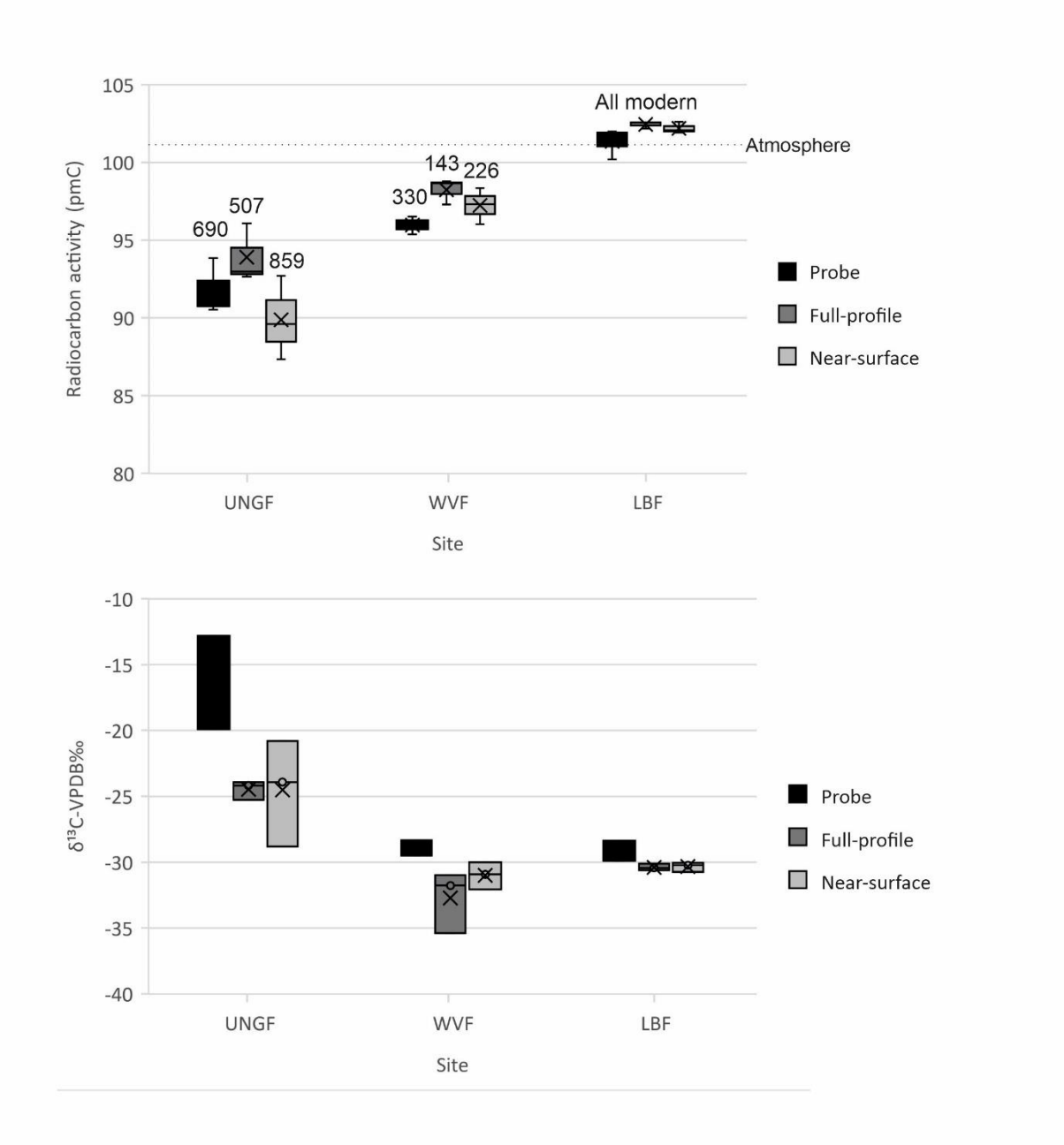


*Figure 4: Variation and median in radiocarbon ages and $\delta^{13}C$ for replicate plots for all experiment types at each site. The average age for experiment types in years BP is displayed above each plot for pMC . When averaging all measurements for each site (replicates and experiment types) the ages are 682 and 232 for UNGF and WVF respectively. LBF ages were all modern (Table 1).*

The radiocarbon results in Table 1 clearly show mineralisation of pre-bomb carbon at two out of three sites for all experiment types, even from near surface sediments. At the site furthest downstream

(LBF), all depths produced only modern carbon (>100 pMC). There were no consistent trends in age in relation to source sediment depth (surface/full-profile/probe) at UNGF or WVF. Surface ages were older than the probe age for two experimental set ups at UNGF, and one experimental set up at WVF. Averaging the replicates at each of these sites, shows that the surface plots were respiring older C at UNGF than the deeper plots (NS: 859 years BP, P: 690 years BP), whereas at WVF, the reverse is true (NS: 226 years BP, P: 330 years BP), but by a lesser degree. The full-profile plots have the youngest age at all sites when the replicates are averaged. When averaging all dates for each site as a whole (all replicates and experiment types), the ages were 682 years BP at UNGF, and 232 years BP at WVF (the ages were all modern at LBF). Therefore, a clear downstream trend in the average age of $CO_2$ production for each source depth is apparent (Table 1 and Figure 4). UNGF produces the oldest $CO_2$, followed by WVF, with only modern $CO_2$ produced at LBF.

*Table 2: The effect size ($\eta^2$) of Site, Type and their interaction expressed as proportion of original variance explained from the two-way ANOVA.*

| Factor/Interaction | Variance of pmC (%) |
|---|---|
| Site | 59 |
| Type | 34 |
| Site*Type | 0 |
| Error | 7 |

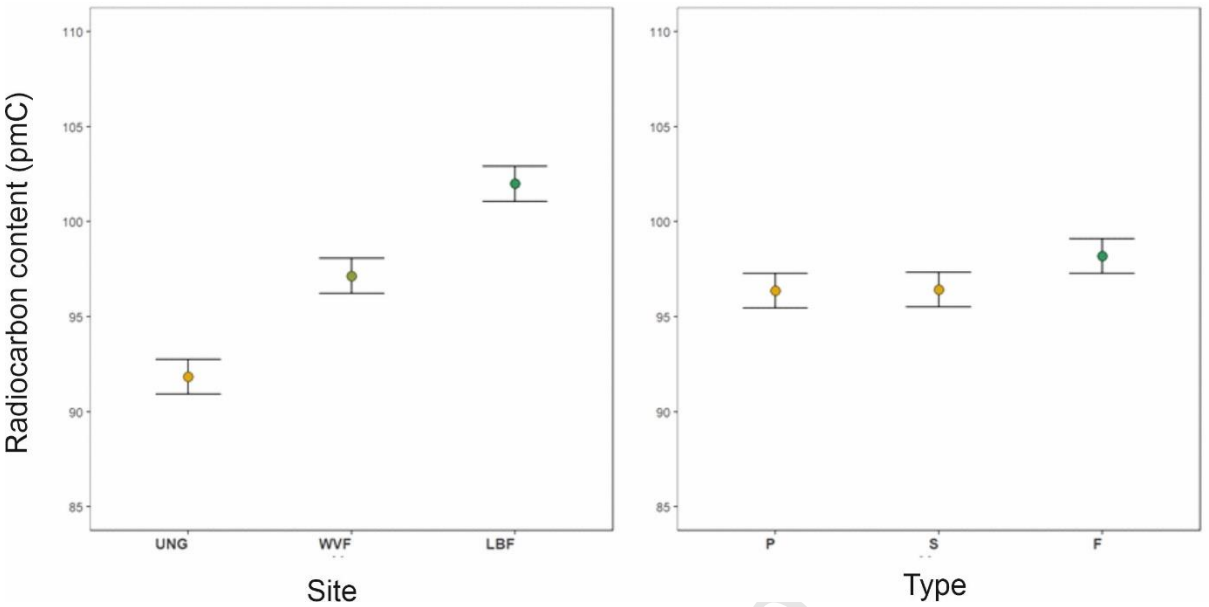


*Figure 5: Main effects plot of marginal means for site (UNGF: 91.9, WVF: 97.2, LBF 102.0) and type (P: 96.4, S: 96.4, F: 98.2) pMC. The standard error on the marginal means is shown- standard error for all is 0.466 pMC.*

The statistical analyses showed that both factors (Site and Type) were significant at $p < 0.05$, but that the interaction between the factors was insignificant. The most important factor was Site, as it explained the majority of the variance in pMC (Table 2). The main effects plot (Figure 5), which displays the marginal means, demonstrates a clear increase in pMC, with distance downstream for the factor Site. With regards to Type, P and S have the same value for the marginal mean and F is the most modern. The pairwise comparisons from the post-hoc Tukey tests, showed that all levels of Site were different from each other, but that only F-P and F-S were significantly different with regards to Type. In order to assess the robustness of the experimental design, we used power analysis to evaluate the type II error and likelihood of rejecting a false null hypothesis. Fisher (1966) suggested that $\beta < 0.8$ indicates that there is a good chance of rejecting the true hypothesis. The power analysis showed that for the Site factor $\beta = 0.98$, so we can reliably interpret these results. However, for the Type factor $\beta = 0.29$, thus these results cannot be treated dependably.

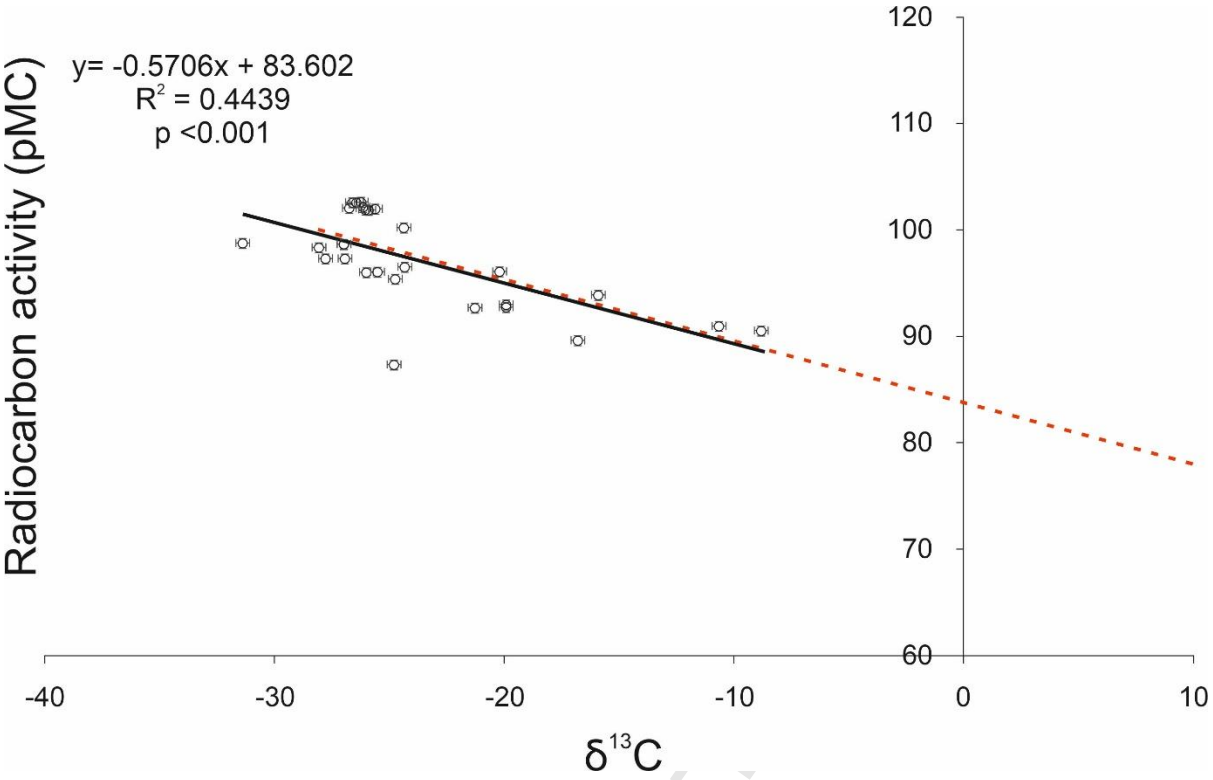


*Figure 6: Relationship between $^{14}C$ (pMC) and $\delta^{13}C$. Black line: regression between the two measures demonstrating a significant correlation. Red dashed line: 2 component isotope mass balance model with end members of a) $CO_2$ derived from recently-fixed OM (100 pMC, $\delta^{13}C$ = -28‰) and b) $CO_2$ associated with methanogenesis (78 pMC, $\delta^{13}C$ = +10‰). See text for more details..*

After correcting for isotopic fractionation during passive trapping (i.e. the addition of 4‰: Garnett et al., 2009), the $\delta^{13}C$ values ranged from -31.4 to -8.8 ‰. Most $\delta^{13}C$ values are around -30 to -25 ‰, which is typical of aerobic decay of C3 organic matter and therefore does not imply significant contributions of atmospheric $CO_2$ ($\delta^{13}C$ -9 ‰; Hemming et al., 2005). $CO_2$ collected at the UNGF site was substantially more $^{13}C$-enriched (e.g., <-20 ‰), however, these results cannot be explained by an atmospheric $CO_2$ contribution, because i) the $^{14}C$ values for these samples are significantly depleted compared to atmospheric $CO_2$, and ii) when the $CO_2$ was most $^{13}C$-enriched, the $CO_2$ trap rates were highest, therefore indicating highest chamber $CO_2$ concentrations (Figure 4; and thus any atmospheric component would be relatively small).

We can explore the source of the $CO_2$ further by plotting the radiocarbon measures against the $\delta^{13}C$ in Figure 6, which demonstrates a significant correlation ($R^2$=0.44, p<0.001). The red dashed line in this Figure is a simple two component isotope mass balance model, adjusted to fit the regression. The

end members of this model are typical of recently fixed C3 OM (ca. 100 pMC and $\delta^{13}C$ = -28‰; <10 years old) and $CO_2$ derived from methanogenesis ($\delta^{13}C$ = +10‰: Clymo and Bryant, 2008). When the pMC of the model was adjusted to track the regression line, 10‰ $\delta^{13}C$ is equivalent to 78 pMC (approximately 2000 years BP). Other potential sources of C do not feature in these results, as there are no data points for geological OM (0 pMC and $\delta^{13}C$ = -20 to -30‰) or geological carbonates (0pMC and $\delta^{13}C$ = 0‰).

The partitioning approach of Estop-Aragones et al., (2018) has previously been used to calculate the contribution of $CO_2$ derived from deeper than the near-surface collars. For successful quantification, $FP^{14}CO_2$ must fall between $NS^{14}CO_2$ and the probe $^{14}CO_2$ value. This partitioning approach fails at most of the replicate plots, because the full profile pMC values do not always satisfy this requirement, resulting in either negative values for the deep peat $CO_2$ contribution, or fractional contributions exceeding 1. The approach was successfully applied at two of the replicate plots at UNGF, and one replicate plot at LBF. The approach was completely unsuccessful at WVF. At UNGF there was no consistent trend, with the majority of $CO_2$ derived from shallow depths in plot 2 (97%) and the opposite ($CO_2$ derived at depth; 80%) for plot 3. In the case of LBF, the majority of $CO_2$ was derived from the surface (98%), which is consistent with the modern radiocarbon dates produced at this site. The partitioning approach on $^{14}CO_2$ gas collection is clearly incompatible in heterogeneous soils, with an aged allochthonous substrate.

## Floodplain stratigraphy

Core imagery, radiography (sediment density) and selected elemental profiles in addition to MSE and the incoherent/coherent scattering ratio are visualised in Figure 7 for UNGF, WVF and LBF. The primary x-rays generated during scanning produce two types of scattering mechanism; Rayleigh (coherent) and Compton (incoherent) scattering. The amount and proportion of the scattering mechanism vary with atomic number, with high OM content favouring the Compton mechanism

(Croudace et al., 2006). As such, higher intensities of incoherent scattering (and higher incoherent/coherent ratios) signal greater organic matter content, with the ratio used as a proxy for OM content (Thomson et al., 2006; Liu et al., 2013; Alderson et al., 2019a). The ratio can therefore assist in corroborating evidence in variations of organic matter content apparent from the visual stratigraphy. The elemental profiles were displayed in peak area and therefore relative to each individual core profile. This is a consequence of the scanning process, as quantitative data is difficult to obtain because of the variations in OM and water content, in addition to particle size, which affects the way the x-rays diffract (Croudace and Rothwell, 2015).

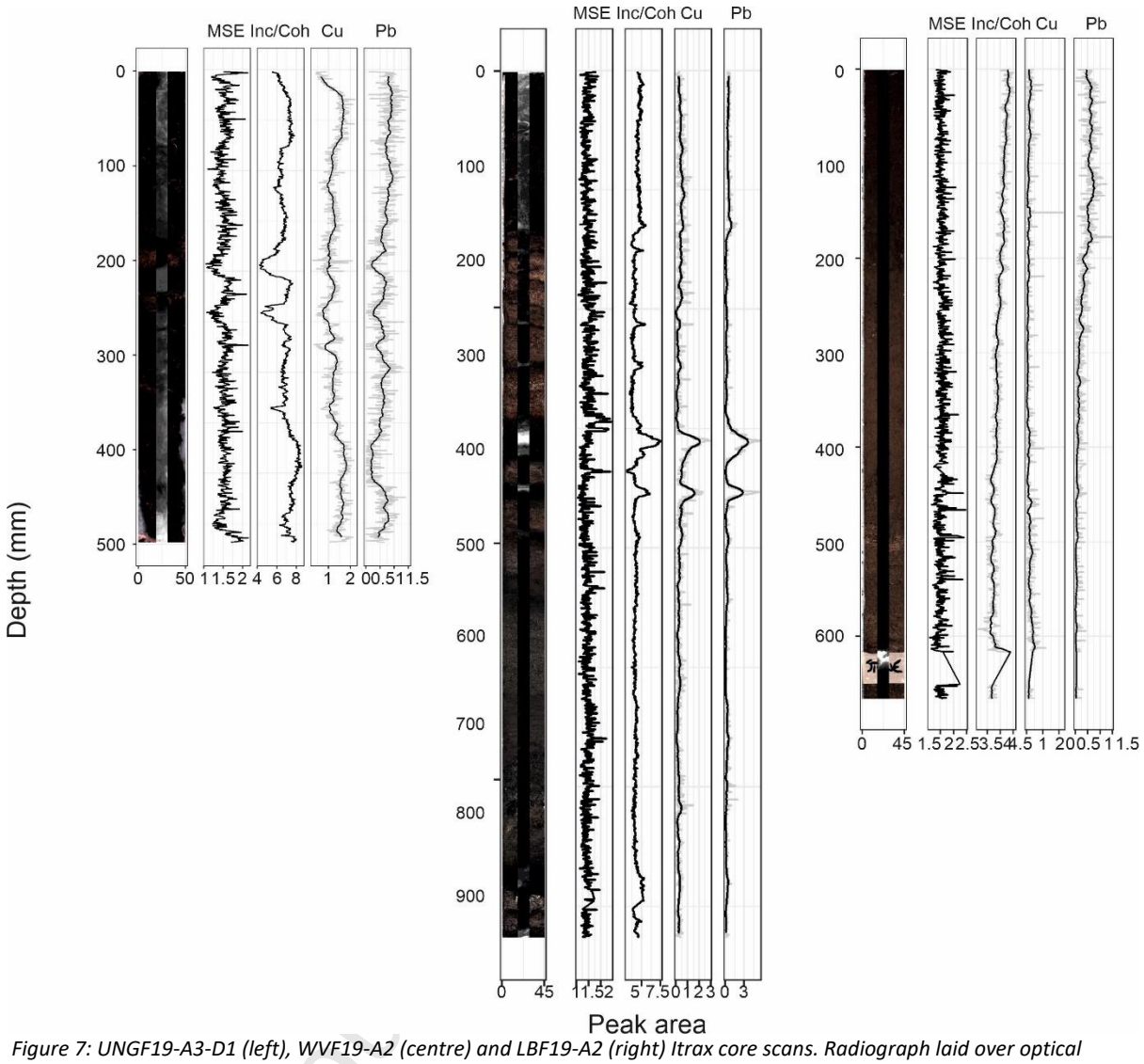


*Figure 7: UNGF19-A3-D1 (left), WVF19-A2 (centre) and LBF19-A2 (right) Itrax core scans. Radiograph laid over optical imagery. Key elements and ratios displayed. MSE is the Mean Square Error and inc/coh is the incoherent/coherent scattering ratio produced by x-ray scanning. The black line is the running mean (20 point) and grey line is the raw data.*

The core stratigraphy for UNGF (Figure 7) demonstrates a number of horizontal mineral bands at approximately 200 mm, 240 mm and 340 mm. These mineral bands coincide broadly with troughs in the incoherent/coherent ratio and suggest that eroded material (with a highly minerogenic load) has been deposited on the floodplain, during a flood event. The Pb record is relatively variable and indicates that deposition has taken place from a mixture of sources from the peatland profile, including portions enriched with Pb. There appears to be a steady increase in Pb from approximately 180 mm to the surface, which may infer more stable in-situ soil development over this timespan.

Aside from the inferences made about the Pb record, it is very difficult to discern differences between OM that is derived from eroded peat, and OM that is derived from floodplain vegetation, because there are not many differences between the original parent materials. This is due to similar environmental conditions, and vegetation community structures between the peatland and floodplain.

The WVF core stratigraphy (Figure 7) is very similar to cores taken previously on this floodplain (see Alderson et al., 2019a for detailed descriptions). There is a thick A-horizon soil at the top of the core, most likely indicating a period of stability for the floodplain with time for in-situ pedogenesis. There are also a number of thin and thicker organic lenses between mineral bands, representing either deposits of organic material from the peatlands during flood events, or in-situ pedogenesis between major flood events. There is most likely a mixture of both of these original organic parent materials. This can be interpreted on the basis of the visual stratigraphy, the density changes in the radiograph, and by variations in the coherent/incoherent ratio. The mineral and organic layers have a generally horizontal structure indicating the likelihood of overbank deposition (Turner et al., 2015). There are two major Pb peaks between approximately 400-450 mm and a minor Pb peak at approximately 150 mm. These Pb peaks also coincide with increases in Cu relative to other parts of the core, inferring the presence of anthropogenic interference in these environments, and are present within organic layers that most likely represent in-situ deposits. They are therefore most likely related to legacy industrial pollution and smelting (Lee and Tallis, 1973; Livett et al., 1979), rather than eroded and contaminated allochthonous material.

The core from the upper section of the Ladybower floodplain (Figure 7) had no obvious organic/minerogenic banding evident from the visual stratigraphy, which is confirmed by the lack of variation of the incoherent/coherent scattering ratio. A gradual colouration change from darker soil to lighter soil downcore was apparent, likely indicating some oxidation of organic contents. Below 500 mm, a coarsening of grain size and visible stones are present. This suggests a change in the nature of

floodplain development below this depth (which could not be captured by the corer), in the form of lateral accretion or large overbank flood events, with the necessary stream power to entrain dense mineral material.

A gradual increase in the relative peak area of Pb is observed towards the top 100 mm of the core. This is consistent with industrial increases of Pb commonly observed in stable sedimentary deposits, including in peatlands (Rothwell et al., 2010), and suggests that the core stratigraphy here is post-1800. Besides the elevated Pb at the top of profile, there is little other elemental variation downcore, suggesting rather stable floodplain forming processes with little external influence, indicating that the Pb peaks here are related to in-situ deposition, rather than Pb bound to eroded OM from the upper catchment.

## Concentrations and fluxes

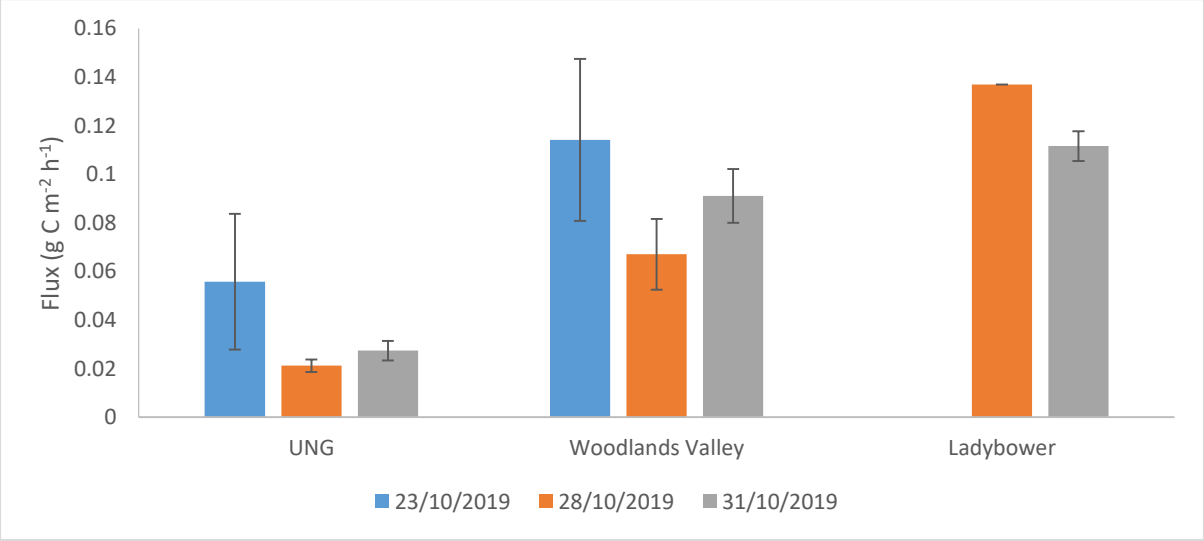


*Figure 8: Respiration flux from replicate plots at each floodplain. The error represents propagated errors from three replicate plots and three replicate measurements per day.*

A limited campaign to take $CO_2$ respiration fluxes from the three floodplains provided relative data on $CO_2$ flux from the three sites, to contextualise other results. Figure 8 shows C respiration fluxes from three replicate plots during October 2019. There is a clear trend of larger respiration fluxes at the

downstream sites. The daily variations demonstrated here, are to be expected on the basis of variations in temperature and water table.

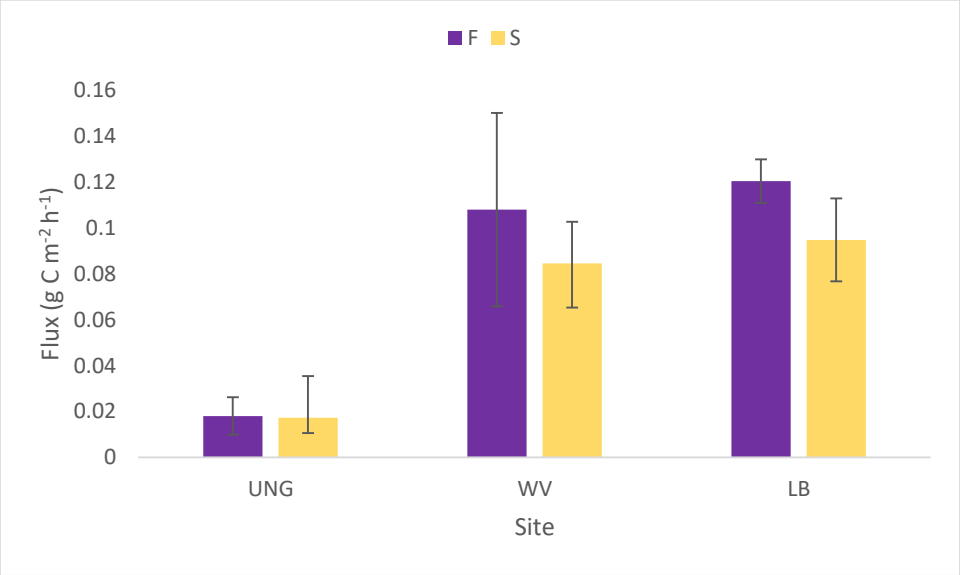


*Figure 9: Fluxes from three replicate plots on a single day within the full-profile and short profile experimental chambers; WV and LB- 05/09/2019, UNG 11/09/2019. Error bars represent propagated error from three replicate plots per site and three replicate measurements at each plot.*

Figure 9 shows the respiration fluxes from a single day from the experimental collars themselves, prior to MSC attachment later in September 2019. There is an increasing downstream trend in the respiration flux, but the clear disparity between UNGF and the other two sites, may be reflective of the waterlogged nature of the UNGF site during the experimental period. This could lead to reduced respiration rates as is typical in peatland landscapes, with water tables intimately linked with the surface (Evans and Warburton, 2007). The fluxes here are small, most noticeably so for UNGF. The actual fluxes here should be interpreted with caution as any drift on the IRGA is more likely to overwhelm the signal, and potentially produce a false result.

The full-profile plots had a greater respiration flux than the short profile plots, as expected on the basis of a greater volume of source OM material available for microbial communities to access. However, it is clear that the upper 250 mm of the floodplain is producing the dominant part of the

total respiration flux, as the short profile bar makes up ~96%, ~78% and ~79% of the total full-profile respiration for UNGF, WVF and LBF respectively.

The UGGA was run for one day in early October 2019 at WVF, with two replicate chambers with 9 cycles each during the course of 5 hours. The average C respiration flux derived from the $CO_2$ component of released floodplain gases was 0.13 ± 0.007 g C $m^{-2}$ $h^{-1}$. The flux decreased over the day, presumably as the temperature decreased. This flux value is similar to the other fluxes taken by the IRGA from both standard collars in the surface of the floodplain and the experimental plots (Figures 8 and 9). The UGGA also measured $CH_4$ respiration fluxes simultaneously but there was no flux present, with concentrations remaining stable through the duration of sampling. The river levels were relatively low on this particular day, so it is unlikely that the floodplain would have experienced any pulse of methane production, although pulses have been measured previously at this site (Alderson, unpublished data from 2015).

# Discussion

The hypotheses outlined in the introduction can be tested by evaluating the results of the various methods from this study. From these observations, and additional contextualising information, we can determine whether the aged C that previous studies have identified has been deposited and processed on floodplains downstream of the eroding headwater peatlands, is being actively turned over at the present day. The discussion will consider the evidence to accept or reject the hypotheses set out in the introduction sequentially, and outline the implications for carbon processes at these sites, before discussing the wider ramifications for floodplain carbon cycling from these results.

## $CO_2$ efflux derived from mineralisation of aged carbon

The average age of the $CO_2$ captured from the three floodplains along the Ashop/Alport system varies. For hypothesis 1 to be accepted, aged OC must be detected in the $^{14}CO_2$ signal as an initial requirement. The $CO_2$ released from the upper two floodplain sites in the catchment is derived from

pre-modern carbon, with average radiocarbon ages of 682 and 232 years at UNGF and WVF respectively, demonstrating that old OC stored in these floodplains was bioavailable to microbial communities present in the floodplain. However, the floodplain site furthest downstream (LBF) does not follow this trend. At LBF, all $^{14}CO_2$ ages for different experimental plots and types were modern. Three potential scenarios are consistent with this result: 1) No aged C from further upstream has been deposited at this site; 2) aged C that has been deposited is not being actively respired here; or 3) that the flux of aged C respired is so minor, that it is completely overwhelmed by the signal from modern soil respiration. At the LBF site, we can be fairly confident that hypothesis 1 should be rejected as the bomb $^{14}C$ ages reflect a post-1950 origin only, although this will be discussed in more detail in a subsequent section.

From the average ages of the organic material alone, hypothesis 1 cannot be definitively accepted or rejected. Ages of at least several hundred years at UNGF and LBF indicate the presence of either older allochthonous sources (if this was the case hypothesis 1 would be accepted), or, aged autochthonous material generated from within the estimated formation development of these floodplains (hypothesis 1 would be rejected). It is important to remember that a single radiocarbon date is a mixture of ages, so it also plausible that both of these possibilities are true, in addition to a component of modern $^{14}CO_2$ in these aged dates. Hypothesis 1 would be rejected even where aged material was being respired if it was sourced in-situ, as this hypothesis relates to a mixture of sources rather than a mixture of ages. Regardless of the original source of this aged $CO_2$ (whether in-situ or allochthonous), aged organic material is being respired, showing that the environmental conditions present on these floodplains during the study period were conducive to mineralisation.

## Is the aged $^{14}CO_2$ produced allochthonous or autochthonous?

The nature of the origin of the aged organic material being respired is important to assess hypothesis 1 and the overall aims of this work. To determine whether aged allochthonous material has been deposited and that aged dates were not simply a function of in-situ organic material generated within

the lifetime of the floodplain, further contextual information on the floodplain history is required; and ideally an accurate date on the formation of these floodplains so that an age cap can be established. Put simply, if the radiocarbon dates from $CO_2$ generated from these floodplains is older than the date of floodplain origin, then at least some of the organic material must originate from elsewhere in the catchment.

Previous work on these floodplains (Evans et al., 2013; Alderson et al., 2019a) provides additional data for the evaluation of hypothesis 1. We can be confident that aged allochthonous C has been deposited and processed on the upper floodplains (UNGF and WVF), based on prior visual evidence of peat block deposition at both sites (author's observations), in addition to radiocarbon dating of organic material in the floodplain stratigraphy at WVF.

At the middle floodplain site, WVF, Alderson et al., (2019a) demonstrated an average age of several organic layers of 3010 years BP, whereas the floodplain age was dated as 500 years old based on two radiocarbon dates of basal wood and a suite of OSL dates. 3010 years BP is much older than the determined age of the upper floodplain stratigraphy, giving confidence that aged material has been deposited and remains present in the floodplain. However in this study, all dates from captured $CO_2$ at WVF are within the lifespan of the floodplain (Table 1). It is possible that the older contribution could be coming from aged in-situ soil deposits rather than allochthonous material. However, several ages older than 250 BP (half the age of the floodplain) tend to suggest the influence of aged allochthonous material, since it is unlikely that carbon turnover is concentrated in the basal sediments, which is supported by the flux data from Figure 8, which suggests that ~78-96% of the flux is coming from the upper sediments. The age of carbon sources yielding $CO_2$ in the near surface (and so recent) horizons is 134 – 326 BP which also indicates a role for the old allochthonous carbon, known to be incorporated into these sediments. As such, we believe that hypothesis 1 can be accepted at WVF.

A similar approach at the upper floodplain site, UNGF, to identify the maximum age of the floodplain is challenging, as the floodplain is hydrologically well connected and subject to frequent deposition events. As such, bulk organic dates would most likely reflect the age of eroded peat, which is not representative of floodplain formation and development, and therefore this material has never been dated. Alderson et al., (2019a) assume that the floodplain formation is a function of the onset of peat erosion, and draws on work from Evans and Lindsay (2010) to calculate this as 500 years BP. There are a number of dates around this age from $CO_2$ released from the floodplain, including one that is younger (UNGF 1F), thus it is reasonable to assume that some of the $CO_2$ flux at this site is derived from in-situ organic material. Older dates (Table 1: up to 1088 years BP) similarly support the idea that allochthonous eroded peat is being respired at this site. Therefore, at UNGF, we can be reasonably confident that hypothesis 1 is supported.

However, at LBF, the dating suggests that predominantly modern autochthonous material is being respired. Indeed, the $^{14}C$ values for respired $CO_2$ at LBF are all very similar to the $^{14}C$ content of $CO_2$ in the contemporary atmosphere (Hammer and Levin, 2017), suggesting that the carbon cycling at this site is dominated, and possibly exclusively, by OM fixed within the last few years. Although we cannot exclude the possibility of aged carbon contributing to $CO_2$ emissions at LBF, the results from our sampling campaign are more consistent with hypothesis 1 being false.

One further consideration to the age and source of $^{14}CO_2$ respired at the sites, is that the roots of the surficial vegetation were not trenched or clipped, and therefore root respiration may also play a role in the modern dates throughout the depth profile at LBF, and indeed, contribute to make the dates younger than they would be, if root respiration could be entirely eliminated at the other sites. Geological sources (both OM and carbonates) contributing significantly to the $CO_2$ emissions can be ruled out, as the mixing model from Figure 6 demonstrates that the regression between $\delta^{13}C$ and $^{14}C$ at all sites (and experiment types), can be explained by two components; recently fixed C3 OM (< 10 years old) or respiration and $CO_2$ derived from methanogenesis from waterlogged periods of

time/sites. In addition, Pawson et al. (2008) found that the total carbon contents of contributions from the underlying geology in Upper North Grain (a small headwater catchment of the River Ashop), ranged from 0.2-2.3%, making it unlikely that geological sources contributed substantially to $CO_2$ emissions. Pedogenic carbonate effects are unlikely in a system with high rainfall and acidic soils.

## Surface versus deep carbon contributions

Assessing hypothesis 2 is critical for aiding our understanding of the internal carbon dynamics within each of the floodplains on the downstream reach. In classical sedimentology, the principle of superposition applies where the oldest deposits are found towards the base of a sediment profile, with gradually younger material towards the surface, as a consequence of the time of deposition. As such, if a floodplain formed with no external organic sediment influences, then we would certainly expect the age of $CO_2$ from the probe measurements to be the oldest, the surface age to be the youngest and the dominant fraction to be from the surface. This is because the most labile fractions from older sedimentary carbon, may have already been utilised by soil microbial communities over the lifespan of the floodplain, with any residual OM typically considered more recalcitrant. The null hypothesis reflects this understanding.

Hypothesis 2 is not supported from the dates in Table 1, as out of the three replicate plots at each site, the near-surface plot type produced the youngest $^{14}C$ age at only one plot each at UNGF and LBF (and at no plots for WVF), with no consistent trends established in terms of age relations between experiment types. Overall, the partitioning approach from Estop-Aragones et al., (2018) failed to proportion the fraction of $^{14}CO_2$ derived from deep or shallow sources at most of the plots (all except three). At LBF, all ages for all experiment types were modern, but the data do suggest that the $^{14}CO_2$ was mainly derived from the uppermost part of the floodplain, adding some tentative support to hypothesis 2.

Using the statistical data to examine depth relationships, the two-way ANOVA and the post-hoc Tukey tests show that FP-P and FP-NS are significantly different, but NS-P are not significantly different. In a

floodplain where external inputs of OM did not play a major role, and there was a linear age-depth relationship, we would expect to see a difference, and arguably the greatest difference between NS and P, as these samples of $CO_2$ would represent the extremes in age in the profile. We would expect the FP sample to be in between the extremes of the most modern (NS) and oldest (P) material if the law of superposition was to apply, and the sediment remained undisturbed post-deposition, as a result of a mixture of modern and aged material.

However, when looking at the averages of pmC (Figure 4), the FP sample is the most modern of all experiment types at every site. On average, at UNGF, the P sample is younger than the NS sample (the opposite to what we would expect), whereas at, WVF and LBF the P sample is older than the NS sample.

Micro-scale variation between replicate plots is not unexpected. Local variations in sediment and nutrient distribution and associated change in microbial communities, are far from unusual across floodplains, and can result in presence/absence of allochthonous sediment deposits, and/or different in-situ vegetation communities across one floodplain, with implications for overall organic content and microbial activity (Craft et al., 2002). The power analysis highlights that the experiment type factor results (the interactions between NS, FP and P described above) cannot be reliably interpreted; there is a good chance of rejecting a true hypothesis and that the sample size for this was too small.

Nevertheless, at UNGF and WVF, aged carbon was clearly mineralised throughout the floodplain profile, resulting in the rejection of hypothesis 2, which has a number of implications. Firstly, at these sites, evidence of pre-modern carbon flux from surface sediments, most likely suggests that aged allochthonous C from elsewhere in the catchment has been deposited at the surface relatively recently, and that this material is being respired, providing evidence consistent with hypothesis 1 at UNGF and WVF. At UNGF, the average age of the P $CO_2$ sample being younger than the NS sample, suggests that there is high connectivity between the floodplain and stream. Eroded, aged material is regularly deposited and actively respired, causing the typical age-depth relationship to be reversed

(although the overlapping error bars should be noted). The River-floodplain connectivity is less pronounced at WVF, and the normal age-depth relationship is more apparent as on average the NS sample is younger than the P sample. However, the fact that the F samples are still the youngest, and that the NS samples are aged, suggests that aged material is present throughout the floodplain.

The second implication is that modern $CO_2$ is produced at depths in excess of 250 mm. Young C generated at the surface through primary productivity, could have migrated into deeper parts of the floodplain (i.e. through root processes, mobile carbon movement through the floodplain, bioturbation, or human activity), further distorting an age-depth signal, along with the recurrent addition of aged material from the upper catchment. Root depths of the most common species on the WVF floodplain (*Nardus Stricta)* can reach depths in excess of 50 cm (Chadwick, 1960), so that there is potential for modern carbon from root exudates, to be introduced at depths below that of our NS sample.

At WVF, water level data in boreholes and their coupling with atmospheric and borehole pressure data (unpublished data, author's own), reflect rising river stage, and demonstrate that the floodplains were permeable. This is consistent with the sandy/silty nature of the deposits garnered from previous work (Alderson et al., 2019a), and the sedimentology featured within Figure 7. Therefore, in addition to the changing aerobic status of the floodplain with rising and falling floodwaters, this provides the opportunity for internal movement of carbon through the floodplain.

Overall, the presence of aged carbon throughout the depth profile, suggests that at the two most upstream sites, the floodplains are relatively well mixed and do not conform to the general principles of superposition. As such, hypothesis 2 is thus disproved at the two upstream sites with the results inconclusive at LBF as the dates were all modern.

## Downstream trends

Hypothesis 3 is clearly supported by a strong downstream trend in the age of $CO_2$ released from floodplain sediments, where the site at the highest point upstream produced the oldest ages, and the site at the furthest point downstream produced the youngest ages (682 years BP > 232 years BP > modern). The ANOVA and post-hoc Tukey tests confirmed that all sites were significantly different from each other. The extremes (UNGF and LBF) were the most different. Aged carbon was produced both upstream and in the middle reach, whereas $^{14}C$ pMC values for LBF suggest that carbon turnover is dominated by fresh carbon (<5-6 years since fixation from the atmosphere), as it is similar or only slightly $^{14}C$-enriched, in comparison to atmospheric $CO_2$. These results allow us to make some inferences about floodplain carbon dynamics along this downstream trajectory.

The evidence presented in relation to hypotheses 1 and 2 is consistent with aged carbon release from reworked organic matter deposited on floodplains during flood events. Conceptually, hypothesis 3 rests on the likelihood that the magnitude of this organic flux decreases downstream, as eroded peat is deposited in zones of intervening storage (upstream floodplains). The declining age of gaseous carbon released from downstream floodplains is consistent with this interpretation, and indicative of a changing balance of modern autochthonous and aged allochthonous carbon in floodplain sediments, so that at the furthest downstream site, respiration of modern allochthonous carbon dominates.

Classic river system theory tells us that from headwaters to lowland systems there are changes in the characteristics of rivers and the valleys that they occupy (Vannote et al., 1980). Sediment loads tend to fine downstream as larger particles are deposited, and increases in river velocity are observed, as channel width widens and total discharge rises (Knighton, 1999). As such, characteristic fluvial landforms change downstream and their residence time in the landscape increases. As the stream velocity increases, if the river does breach the floodplain surface, POM may not settle because it is more likely to continue to be entrained, flow over the floodplain surface in the floodwaters and reconnect with the river channel as the settling velocity is not reached.

Pawson et al., (2012) showed declining loads of POC downstream of headwater peatlands, in the same area as this study. Evans et al., (2022) have also found aged POC in the headwaters of the River Ashop (circa 2000-3000 years BP). The findings of this study are consistent with this pattern and with increasing dilution of peat derived OM downstream, as the proportion of the floodplain catchment that has other soil types increases. The sedimentary evidence at the sites (characterised by repeating units of horizontally stratified organic and mineral sediments) in this study, indicates the dominance of vertical accretion by overbank deposition in the initial formation of the floodplains, regardless of reach position. This is most apparent in the core stratigraphy's at UNGF and WVF. At LBF, the sediments are more homogeneous within the surface cores, but deeper sediments exposed at the river's edge (not captured by coring) at this site, show evidence of vertical accretion in the form of horizontal layers of mineral and organic material, very similar to those observed at WVF. If the organic material in the deeper sediments is redeposited peat, this site has clearly experienced different geomorphological processes more recently, and if there is continued mineralisation of this material, it is overwhelmed by respiration of more-modern material. As such, it is important to examine the differences in the sedimentary contexts and particularly the geomorphic setting of the three sites in more detail individually, which may further explain the patterns of carbon turnover observed down the system.

### UNGF

The sedimentary sequence at UNGF is organic rich. This site is within the margins of a severely eroded peatland (as described in Evans et al., 2006). Fine peat is observed to be deposited on the floodplain, together with large blocks of peat eroded from upstream gully edges. Large peat blocks may be mobilised (Boothroyd and Warburton, 2020) and deposited on floodplains in headwater peatlands and incorporated into floodplain sediments (Warburton and Evans, 2011). Their incorporation into the floodplain stratigraphy could result in carbon sequestration and metre scale variation in carbon sink/source status across the uppermost reaches of headwater peatlands. The travel of these peat

blocks is limited to a maximum of ~120 m, dependent on size and shape according to Boothroyd and Warburton (2020). Therefore, some of the OM load from eroded headwaters, may never reach floodplains further downstream, as it has already been deposited and processed within floodplains close to the source of erosion, as at UNGF. Deposited peat blocks are commonly seen on the well-connected floodplain surfaces of UNGF. The site photograph in Figure 1, clearly shows the floodplain surface and stream are intimately connected with wetland vegetation present.

The organic rich sediments and high water tables observed at UNGF, are also consistent with an important role for anaerobic decomposition of OM at this site. The $\delta^{13}C$ content of $CO_2$ can be used to determine the principal pathways of $CO_2$ production (Charman et al., 1999). The $\delta^{13}C$ results indicate that the samples from UNGF were highly $^{13}C$-enriched, suggesting anaerobic decay was taking place, resulting in $^{13}C$-enriched $CO_2$ (e.g., Clymo and Bryant, 2008). We also observed that the water table was at or close to the surface for most of the sampling period at the UNGF site, thus providing conditions that would favour methanogenesis. This was most clearly seen in the probe samples at this site. As the water table was at or close to the surface for the duration of the experiment, the probes were likely below the water table all of the time, hence they show the best evidence of methanogenesis from the $\delta^{13}C$ results. The samples derived from the chambers (FP and NS), are likely to not be as $^{13}C$ enriched, as there would be a greater $CO_2$ component derived from aerobic decay when the water table was not at the surface.

### WVF

WVF is a well-defined meandering floodplain system beyond the limit of the peatland. This floodplain is believed to have formed by vertical accretion in response to elevated sediment loads, associated with upstream peat erosion. Floodplain connectivity is reduced in comparison to UNGF, with overbank flows observed only occasionally at present-day (Alderson et al., 2019a). The stratigraphy however is consistent with ongoing periodic inundation of the floodplain and associated deposition of mineral material and allochthonous organic carbon. The wetland vegetation present in the site photo

in Figure 1 (although there is an absence of mosses), demonstrate that the floodplain remains connected, although not at the same frequency as at UNGF.

LBF

In line with the decreasing POM loads downstream (e.g. Pawson et al. 2012), some POC may either never reach the floodplain surfaces of the lower catchment or be re-entrained and continue the downstream journey, and in this location possibly settle in Ladybower reservoir. Stimson et al., (2017) highlight that reservoirs in this region can act as hotspots of carbon turnover, as a consequence of high POC loads and long water residence times.

The upper sediments of LBF do not appear to be connected to present-day river dynamics and because of the geomorphic context here, this part of the system appears to be acting as more of a 'pipe', as the floodplain height is restrictive to overbank flow. This is apparent through several lines of evidence. Firstly in Figure 6, there is no indication of the couplets consisting of minerogenic material and an organic cap (Turner et al., 2015), typically seen in river floodplains where overbank deposition is the dominant accretional process (as observed in UNGF and WVF). Secondly, the increasing Pb concentration profile towards the surface indicates that for at least a century, autochthonous sedimentation appears to have dominated, based on the introduction of leaded petrol into the environment, demonstrating a different age profile to the two upper sites. Thirdly, this is supported by the vegetation type shown in the site photograph in Figure 1; some tree species and common grassland, whereas there is no wetland vegetation like the upper sites. Through these lines of evidence, the present-day floodplain appears to be relatively stable. Extreme events, in theory could breach the floodplain surface, but the sediment grain size at this point downstream is likely to be finer and restrictive to trapping OM.

However, this does not mean that this part of the system has never in it's history received deposition of peat-derived OM. In fact, observational evidence of regular sequential layers from the exposed riverbank indicates otherwise. The modern turnover of $^{14}C$ suggests a few different possible scenarios;

any aged organic material at depth in the floodplain is physically isolated from active microbial communities (Berhe et al., 2007), or, that the signal of any aged C that is being turned over is overwhelmed by modern day respiration. Respiration of modern OC is also likely to have occurred from the upper soils of UNGF and WVF, as there are clear A horizon soils here, but in contrast to LBF, the respiration signal from aged C dominates. Root respiration may certainly have a role here, as the roots were not clipped, and were likely to extend into deeper parts of the floodplain contributing to modern dates at depth.

Over a distance of 10 km downstream there is significant change in the nature of the floodplain systems studied. The observed patterns of radiocarbon age of OM mineralisation are consistent with a transition from headwater floodplains dominated by overbank deposition of allochthonous carbon from the eroding peatlands, to less well-connected floodplains above Ladybower reservoir, where modern autochthonous carbon dominates carbon loss from the floodplain.

## Lateral transfers and lability

The observations presented in this study which show aged organic material is being respired in these environments are pertinent to the developing debates around inherent recalcitrance versus environmental conditions, as controls on the preservation/mineralisation of OM (Schmidt et al., 2011; Lehmann and Kleber, 2015). Fresh primary production at the floodplain surface is labile and potentially rapidly respired. Old carbon reworked from peatland storage would commonly be viewed as less labile, since the peat entering storage below the water table in functioning peatlands is the residual OM that survives initial litter decomposition at the peatland surface. The evidence presented here suggests that as this material is translocated from an anaerobic environment to the more transiently aerobic conditions of a permeable floodplain, this aged material is actively respired suggesting it is relatively reactive under these conditions. This is supported by our limited gas flux data (Figure 9) which suggested ~78-96% of $CO_2$ emissions originated from the surface. Although we must be careful from inferring too much from this data as it only represents a single day per site.

Increasingly, the literature is moving away from the idea of inherent recalcitrance of some organic matter compounds (e.g., lignins) and has focused attention on sediment character within a particular landform and the environmental conditions imposed on the organic matter contained within that landform (von Lützow et al., 2006). In the context of floodplain environments, swift burial of deposited organic carbon (either autochthonous soil or allochthonous delivery of OM) may reduce post-depositional diagenesis over the short-term. Where there are sediment units with both organic and mineral material, organo-mineral associations have the potential to increase carbon storage potential (von Lützow et al., 2006) and protect OM beyond the storage timescales of landforms (Hemingway et al., 2019).

However, clear evidence from this study suggests that allochthonous OM originating from eroding peatlands, that is subsequently deposited and buried as soil horizons in extreme headwater floodplains, is still available to microbial communities years after the deposition event. This does not take into account any rapid mineralisation that may take place immediately after deposition on the floodplain surface.

The observation from the gas flux measurements, that quantitatively near surface horizons dominate the flux of $CO_2$ from the floodplain, and the fact that we observe old $CO_2$ being emitted from our near surface measurement, suggest that significant quantities of old carbon are being mineralised in this zone. This implies that eroded peat deposited on the floodplain surface is readily mineralised in the aerobic environment, which is consistent with the view that environment dominates over lability as a control on mineralisation rates.

The observation of mineralisation of peat in our headwater sites is an important insight, indicating that floodplains in a relatively narrow halo (in this watershed <8 km) around degrading peatland systems are potentially important sites of carbon turnover, and more work is required to fully characterise the carbon balance of these sites.

The environmental conditions in the peatland headwaters are conducive not only to peat growth, but also to OM preservation because of regular high water tables and cold, wet conditions. Floodplains are characteristically wet as they are periodically inundated and nutrient rich, with primary productivity relatively high (Opperman et al., 2010). However, they also tend to be sites of frequent disturbance due to event-related erosion, and low water conditions (common in flashy peatland streams) lead to periodic aeration of the floodplain. Soil microbial communities can rapidly respond to changes in local conditions, enabling floodplains that are normally carbon sinks to become temporary carbon sources. The results presented here suggest that allochthonous OM is bioavailable, and in some floodplains may represent a carbon source over longer time periods.

## Implications for carbon budgets and floodplain functioning

Hoffmann et al., (2013) argue that carbon storage in the headwaters is limited by the short residence time of sediment, whereas lowland floodplains have the potential to be large carbon sinks. Similarly, Sutfin et al., (2016) argue that the optimum conditions for carbon preservation in floodplains is cold, wet environments, where the valley width is wide and channel system is complex, and aggradation is favoured over erosion; the majority of these factors are more likely in lowland environments.

In this study, we have shown that old carbon is turned over in floodplain systems that have been stable on the order of 500 years, in a cool, wet, temperate environment. Alderson et al., (2019a) showed that carbon storage in these floodplains represented 0.8-4.5% of estimated sediment flux. The evidence of old carbon turnover in these systems, suggests that this relatively low storage potential is related not only to the proportion of the OM flux stored in the floodplain systems, but also to in-situ carbon loss from sites that are actively cycling carbon. Scheingross et al., (2021) show that in lowland floodplains in Argentina, up to 80% of POC is mineralised within millennial timescales, so it appears that even in sites where conditions appear to favour carbon storage, it may be more appropriate to consider floodplains as hotspots of carbon turnover than passive stores.

Additional information is required to understand whether the aged carbon released from these floodplains is significant in the context of the overall carbon budget (sink versus source). Limited respiration fluxes from the sites, demonstrate a clear increasing downstream trend in carbon mineralisation, but this study did not address NEE, or fully account for other greenhouse gases (particularly $CH_4$ in relation to the interesting $\delta^{13}C$ results). Clearly, further work is required here to understand the magnitude of aged carbon release in these environments.

The significance of these results and the relevance and application in other environments with peat-based soils must be considered, as headwater catchments in temperate zones have distinct characteristics that might not be widely transferrable. The erosion of headwater peatland landscapes and lowered water tables (and thus changing acrotelm/catotelm boundary), and, the thawing of permafrost soils that have previously been frozen for thousands of years as a consequence of warmer, wetter conditions in the Arctic, both result in previously inaccessible C (or at reduced rates), becoming accessible to microbial communities.

Increased fluvial discharges as a result of climate change may also cause lateral erosion and redistribution of previously locked up OC, below the depth of annual thaw (Vonk et al., 2019). However, Douglas et al., (2022) found that in the Koyukuk River, organic carbon re-deposition in adjacent point bars dampened positive feedback from POC released by river erosion. It is possible that narrow halos will be formed around floodplains, with significant stores of erodible OM in the Arctic if comparable to this study, but this warrants further attention. It is important to study large rivers as their OC dynamics reflect spatial and temporal scales that can be linked to global cycling (Torres et al., 2017).

## Conclusions

Where the upper catchments that supply allochthonous carbon to floodplains are degrading, the floodplain carbon store will include old carbon reworked from elsewhere. Peatlands in the British

uplands are an extreme case of degrading systems with a high organic river load. The understanding of OM dynamics in headwater floodplains reported here, in the context of eroding peatlands, contributes to understanding the fate of carbon in these environments, but can also inform what may happen in other areas that are vulnerable to severe erosion as a consequence of climate change and other pressures (e.g., land use changes, pollution), and have the potential to produce high organic sediment loads (e.g., permafrost regions- Schuur et al., 2015; Turetsky et al., 2019).

Further work is required to contextualise the loss of old carbon in the full carbon budget of these headwater peatlands. However, this study has shown that in degrading peatland catchments where allochthonous old carbon is a significant part of sediment flux, floodplains are sites of turnover of old carbon. Reworked carbon is not transported passively through the sediment system, but is actively turned over in contexts where environmental conditions support microbial decomposition. This applies even when the influx of OM is apparently recalcitrant material. In this study, old carbon was being released across the full extent of the floodplain sediment profile.

The evidence reported here suggests that the importance of headwater floodplains as hotspots of old carbon turnover declines rapidly downstream. It is argued that this pattern is geomorphologically controlled. Floodplain environments support microbial communities capable of respiring aged OM, but the supply of allochthonous OM to floodplains decreases downstream due to upstream deposition.

Understanding the full carbon budget of peatland systems requires an understanding of the fate of particulate carbon which is eroded from degrading peatlands. The evidence presented here points to a landscape scale hotspot of old carbon turnover, in a narrow band marginal to the boundaries of eroding peatland systems. These peat marginal headwater floodplains are sites of carbon turnover, so that a proportion of the particulate carbon lost to the fluvial system, must be regarded as a carbon loss to the atmosphere. Further work is required to quantify this relation.

## Acknowledgements

The authors would like to thank Sarah Brown, Martin Kay, Tom Bishop, John Moore and Benjamin Bell, all of the University of Manchester for their assistance with the various aspects of fieldwork for this project. We would also like to thank Tom Bishop for his help with core scanning and writing code in R to produce diagrams for this work. We would also like to thank Adam Johnston for his assistance in creating a map and a number of anonymous reviewers whose comments improved the manuscript substantially. This project was supported by NERC via NEIF Radiocarbon NRCF010001 allocation number 2176.0319, and a grant from the Early Career Research Support Fund from the School of Environment, Education and Development, University of Manchester.

## References

Alderson, D. M., Evans, M. G., Rothwell, J. J., Rhodes, E. J., Boult, S., 2019a. Geomorphological controls on fluvial carbon storage in headwater peatlands. Earth Surface Processes and Landforms 44, 1675–1693. https://doi.org/10.1002/esp.4602.

Alderson, D. M., Evans, M. G., Shuttleworth, E. L., Pilkington, M., Spencer, T., Walker, J., Allott, T. E. H., 2019b. Trajectories of ecosystem change in restored blanket peatlands. Science of the Total Environment, 665, 785-796. https://doi.org/10.1016/j.scitotenv.2019.02.095.

Anderson, T.W., Darling, D.A., 1952. Asymptotic theory of certain “goodness-of-fit” criteria based on stochastic processes. Annals of Mathematical Statistics, 23, 193–212.

Aufdenkampe, A.K., Mayorga, E., Raymond, P.A., Melack, J.M., Doney, S.C., Alin, S.R., Aalto, R.E., Yoo, K., 2011. Riverine coupling of biogeochemical cycles between land, oceans, and atmosphere. Frontiers in Ecology and the Environment, 9 (1), 53-60. https://doi.org/10.1890/100014

Battin, T.J., Luyssaert, S., Kaplan, L.A., Aufdenkampe, A.K., Richter, A., Tranvik, L.J., 2009. The boundless carbon cycle. Nature Geoscience, 2, 598-600. https://doi.org/10.1038/ngeo618

Battin, T.J., Kaplan, L.A., Findlay, S., Hopkinson, C.S., Marti, E., Packman, A.I., Newbold, J.D., Sabater, F., 2008. Biophysical controls on organic carbon fluxes in fluvial networks. Nature Geoscience 1, 95–100. https://doi.org/10.1038/ngeo101.

Berhe, A.A., Harte, J., Harden, J.W., Torn, M.S., 2007. The significance of the erosion-induced terrestrial carbon sink. BioScience, 57 (4), 337-346. https://doi.org/10.1641/B570408

Bertoni, G., Ciuchini, C., Tappa, R., 2004. Measurement of long-term average carbon dioxide concentrations using passive diffusion sampling. Atmospheric Environment 38 (11), 1625-1630. https://doi.org/10.1016/j.atmosenv.2003.12.010

Bishop, T., 2021. itraxR: Itrax Data Analysis Tools. R package version 1.1. https://CRAN.R-project.org/package=itraxR

Boothroyd, R. J., Warburton, J., 2020. Spatial organisation and physical characteristics of large peat blocks in an upland fluvial peatland ecosystem. Geomorphology 370. https://doi.org/10.1016/j.geomorph.2020.107397

Chadwick, M. J., 1960. Nardus Stricta L. Journal of Ecology, 48(1), 255–267. https://doi.org/10.2307/2257324

Charman, D.J., Aravena, R., Bryant, C.L., Harkness, D.D., 1999. Carbon isotopes in peat, DOC, CO2, and CH4 in a Holocene peatland on Dartmoor, southwest England. Geology 27, 539–542. https://doi.org/10.1130/0091-7613(1999)027%3C0539:CIIPDC%3E2.3.CO;2

Clay, G.D. and Evans, M.G., 2017. Ten-year meteorological record for an upland research catchment near the summit of Snake Pass in the Peak District, UK. Weather, 72: 242-249. https://doi.org/10.1002/wea.2824

Clymo, R. S., Bryant, C. L., 2008. Diffusion and mass flow of dissolved carbon dioxide, methane, and dissolved organic carbon in a 7-m deep raised peat bog. Geochimica et Cosmochimica Acta 72 (8), 2048-2066. https://doi.org/10.1016/j.gca.2008.01.032

Cole, J.J., Prairie, Y.T., Caraco, N.F., McDowell, W.H., Tranvik, L.J., Striegl, R.G., Duarte, C.M., Kortelainen, P., Downing, J.A., Middelburg, J.J., Melack J., 2007. Plumbing the global carbon cycle: Integrating inland waters into the terrestrial carbon budget. Ecosystems 10: 171–184. https://doi.org/10.1007/s10021-006-9013-8.

Craft, J.A., Stanford, J.A., Pusch, M., 2002. Microbial respiration within a floodplain aquifer of a large gravel-bed river. *Freshwater Biology* 47 (2): 251-261. https://doi.org/10.1046/j.1365-2427.2002.00803.x

Croudace, I.W., Rindby, A., Rothwell, R.G., 2006. ITRAX: description and evaluation of a new multi-function X-ray core scanner. Geological Society, London, Special Publications, 267, 51-63. https://doi.org/10.1144/GSL.SP.2006.267.01.04

Croudace, I.W., Rothwell, R.G., (Eds.) 2015. Micro-XRF Studies of Sediment Cores: Applications of a non-destructive tool for the environmental sciences. Dordrecht, Springer.

Douglas, M. M., Li, G. K., Fischer, W. W., Rowland, J. C., Kemeny, P. C., West, A. J., Schwenk, J., Piliouras, A. P., Chadwick, A. J., Lamb, M. P., 2022. Organic carbon burial by river meandering partially offsets bank erosion carbon fluxes in a discontinuous permafrost floodplain, Earth Surface Dynamics, 10, 421–435. https://doi.org/10.5194/esurf-10-421-2022.

Estop-Aragonés, C., Cooper, M. D. A., Fisher, J. P., Thierry, A., Garnett, M. H., Charman, D. J., Murton, J. B., Phoenix, G. K., Treharne, R., Sanderson, N. K., Burn, C. R., Kokelj, S. V., Wolfe, S. A., Lewkowicz, A. G., Williams, M., Hartley, I. P., 2018. Limited release of previously-frozen C and increased new peat formation after thaw in permafrost peatlands. Soil Biology & Biochemistry, 118, 115-129. https://doi.org/10.1016/j.soilbio.2017.12.010

Evans, M., Warburton, J., Yang, J., 2006. Eroding blanket peat catchments: Global and local implications of upland organic sediment budgets. Geomorphology, 79 (1-2), 45-57. https://doi.org/10.1016/j.geomorph.2005.09.015

Evans, C., Allott, T., Billett, M., Burden, A., Chapman, P., Dinsmore, K., Evans, M., Freeman, C., Goulsbra, C., Holden, J., Jones, D., 2013. Greenhouse gas emissions associated with non gaseous losses of carbon from peatlands–Fate of particulate and dissolved carbon. Final Report to the Department for Environment, Food and Rural Affairs, Project SP1205. Centre for Ecology and Hydrology, Bangor

Evans, M. G., Alderson, D. M., Evans, C. D., Stimson, A., Allott, T. E. H., Goulsbra, C., Worrall, F., Crouch, T., Walker, J., Garnett, M. G., Rowson, J., 2022. Carbon loss pathways in degraded peatlands: New insights from radiocarbon measurements of peatland waters. Journal of Geophysical Research, Biogeosciences, 127, e2021JG006344. https://doi.org/10.1029/2021JG006344

Evans, C. D., Page, S. E., Jones, T., Moore, S., Gauci, V., Laiho, R., Hruška, J., Allott, T. E. H., Billett, M. F., Tipping, E., Freeman, C., Garnett, M. H., 2014. Contrasting vulnerability of drained tropical and high-latitude peatlands to fluvial loss of stored carbon. Global Biogeochemical Cycles, 28(11), 1215-1234. https://doi.org/10.1002/2013GB004782

Evans, M., Lindsay, J., 2010. The impact of gully erosion on carbon sequestration in blanket peatlands. Climate Research, 45 (1), 31-41.

Evans, M.G., Warburton, J., 2007. Geomorphology of upland peat: Erosion, form and landscape change. Oxford, Blackwell.

Fisher, R.A., 1966. The design of experiments. 8th edition. Hafner :Edinburgh.

Galy, V., Eglinton, T., 2011. Protracted storage of biospheric carbon in the Ganges-Brahmaputra basin. Nature Geoscience 4, 843-847. https://doi.org/10.1038/ngeo1293

Garnett, M.H., Hartley, I.P., Hopkins, D.W., Sommerkorn, M., Wookey, P.A., 2009. A passive sampling method for radiocarbon analysis of soil respiration using molecular sieve. Soil Biology and Biochemistry, 41(7), 1450-1456. https://doi.org/10.1016/j.soilbio.2009.03.024

Garnett, M. H. , Newton, J.-A., Ascough, P. L., 2019. Advances in the radiocarbon analysis of carbon dioxide at the NERC radiocarbon facility (East Kilbride) using molecular sieve cartridges. Radiocarbon 61 (6), 1855-1865. https://doi.org/10.1017/RDC.2019.86

Garnett, M.H., Hardie, S.M.L., 2009. Isotope (14C and 13C) analysis of deep peat CO2 using a passive sampling technique. Soil Biology and Biochemistry 41 (12), 2477-2483. https://doi.org/10.1016/j.soilbio.2009.09.004

Garnett, M.H., Hartley, I.P., 2010. A passive sampling method for radiocarbon analysis of atmospheric CO2 using molecular sieve. Atmospheric Environment 44 (7), 877-883. https://doi.org/10.1016/j.atmosenv.2009.12.005

Goulsbra, C.S., Evans, M.G., Allott, T.E.H., 2016. Rates of $CO_2$ efflux and changes in DOC concentration resulting from the addition of POC to the fluvial system in peatlands. *Aquatic Sciences* **78,** 477–489. https://doi.org/10.1007/s00027-016-0471-6

Hammer, S., Levin, I., 2017. Monthly mean atmospheric D14CO2 at Jungfraujoch and Schauinsland from 1986 to 2016. heiDATA, V2. https://doi.org/10.11588/data/10100.

Hardie, S.L., Garnett, M.H., Fallick, A.E., Rowland, A.P., Ostle, N.J., 2005. Carbon dioxide capture using a zeolite molecular sieve sampling system for isotopic studies (13C and 14C) of respiration. Radiocarbon 47(3), 441-451. https://doi.org/10.1017/S0033822200035220

Hemingway, J. D., Rothman, D. H., Grant, K. E., Rosengard, S. Z., Eglinton, T. I., Derry, L. A., Galy, V. V., 2019. Mineral protection regulates long-term global preservation of natural organic carbon. Nature, 570, 228-231. https://doi.org/10.1038/s41586-019-1280-6

Hemming, D., Yakir, D., Ambus, P., Aurela, M., Besson, C., Black, K., Buchmann, N., Burlett, R., Cescatti, A., Clement, R., Gross, P., Granier, A., Grunwald, T., Havrankova, K., Janous, D., Janssens, I. A., Knohl, A., Ostner, B. K., Kowalski, A., Laurila, T., Mata, C., Marcolla, B., Matteucci, G., Moncrieff, J., Moors, E. J., Osborne, B., Pereira, J. S., Pihlatie, M., Pilegaard, K., Ponti, F., Rosova, Z., Rossi, F., Scartazza, A.,

Vesala, T., 2005. Pan-European delta C-13 values of air and organic matter from forest ecosystems. Global Change Biology 11(7): 1065-1093. https://doi.org/10.1111/j.1365-2486.2005.00971.x

Hoffmann, T., Glatzel, S., Dikau, R., 2009. A carbon storage perspective on alluvial sediment storage in the Rhine catchment. Geomorphology 108, 127–137. https://doi.org/10.1016/j.geomorph.2007.11.015

Hoffmann, T., Schlummer, M., Notebaert, B., Verstraeten, G., Korup, O., 2013. Carbon burial in soil sediments from Holocene agricultural erosion, Central Europe. Global Biogeochemical Cycles 27, 828–835. https://doi.org/10.1002/gbc.20071.

Hope, D., Billet, M. F., Cresser, M. S., 1997. Exports of organic carbon from two river systems in NE Scotland, Journal of Hydrology, 193, 61–82. https://doi.org/10.1016/S0022-1694(96)03150-2

Knighton, A.D., 1999. Downstream variation in stream power. Geomorphology 29 (3-4): 293-306. https://doi.org/10.1016/S0169-555X(99)00015-X

Lee, J., Tallis, J., 1973. Regional and historical aspects of lead pollution in Britain. *Nature* **245,** 216-218. https://doi.org/10.1038/245216a0

Lehmann, J., Kleber, M., 2015. The contentious nature of soil organic matter. Nature, 528 (7580), 60-68. https://doi.org/10.1038/nature16069

Lininger, K. B., Wohl, E., Rose, J. R., Leisz, S. J., 2019. Significant floodplain soil organic carbon storage along a large high-latitude river and its tributaries. Geophysical Research Letters 46, 2121-2129. https://doi.org/10.1029/2018GL080996

Liu, X., Colman, S.M., Brown, E.T., Minor, E.C., Li, H., 2013. Estimation of carbonate, total organic carbon, and biogenic silica content by FTIR and XRF techniques in lacustrine sediments. Journal of Paleolimnology, 50, 387-398. https://doi.org/10.1007/s10933-013-9733-7

Livett, E., Lee, J., Tallis, J., 1979. Lead, Zinc and Copper analyses of British blanket peats. *Journal of Ecology, 67*(3), 865-891. https://doi.org/10.2307/2259219

Lloyd, J., Taylor, J. A., 1994. On the temperature dependence of soil respiration. Functional Ecology, 8(3), 315–323. https://doi.org/10.2307/2389824

McClain, M. E., Boyer, E. W., Dent, L., Gergel, S. E., Grimm, N. B., Groffmann, P. M., Hart, S. C., Harvey, J. W., Johnston, C. A., Mayorga, E., McDowell, W. H., Pinlay, G., 2003. Biogeochemical hot spots and hot moments at the interface of terrestrial and aquatic ecosystems. Ecosystems 6 301-312. https://doi.org/10.1007/s10021-003-0161-9

Opperman, J. J., Luster, R., McKenney, B. A., Roberts, M., Meadows, A. W., 2010. Ecologically functional floodplains: Connectivity, flow regime, and scale. *Journal of the American Water Resources Association* 46 (2): 211-226. https://doi.org/10.1111/j.1752-1688.2010.00426.x.

Pawson, R. R., 2008. Assessing the role of particulates in the fluvial organic carbon flux from eroding peatland systems. University of Manchester, Manchester, UK.

Pawson, R.R., Evans, M.G., Allott, T.E.H.A., 2012. Fluvial carbon flux from headwater peatland streams: Significance of particulate carbon flux. Earth Surface Processes and Landforms, 37 (11), 1203-1212. https://doi.org/10.1002/esp.3257

Rothwell, J. J., Taylor, K. G., Chenery, S. R. N., Cundy, A. B., Evans, M. G., Allott, T. E. H., 2010. Storage and behavior of As, Sb, Pb, and Cu in ombrotrophic peat bogs under contrasting water table conditions. Environmental Science & Technology 44 (22), 8497-8502. https://doi.org/10.1021/es101150w

Scheingross, J. S., Repasch, M. N., Hovius, N., Sachse, D., Lupker, M., Fuchs, M., Halevy, I., Gröcke, D. R., Golombek, N. Y., Haghipour, N., Eglinton, T. I., Orfeo, O., Schleicher, A. M., 2021. The fate of fluvially-deposited organic carbon during transient floodplain storage. Earth and Planetary Science Letters 561, 116822. https://doi.org/10.1016/j.epsl.2021.116822

Schmidt, M.W.I., Torn, M.S., Abiven, S., Dittmar, T., Guggenberger, G., Janssens I. A., Kleber, M., Kogel-Knaber, I., Lehmann, J., Manning, D. A. C., Nannipieri, P., Rasse, D. P., Weiner, S., Trumbore, S. E., 2011. Persistence of soil organic matter as an ecosystem property. Nature 478: 49-56. https://doi.org/10.1038/nature10386

Schuur, E. A. G., McGuire, A. D., Schädel, C., Grosse, G., Harden, J. W., Hayes, D. J., Hugelius, G., Koven, C. D., Kuhry, P., Lawrence, D. M., Natali, S. M., Olefeldt, D., Romanovsky, V. E., Schaefer, K., Turetsky, M. R., Treat, C. C., Vonk, J. E., 2015. Climate change and the permafrost carbon feedback. Nature, 520(7546), 171–179. https://doi.org/10.1038/nature14338

Stimson, A.G., Allott, T.E.H., Boult, S., Evans, M.G., 2017. Reservoirs as hotspots of fluvial carbon cycling in peatland catchments. Science of the Total Environment 15, 580: 398-411. https://doi.org/10.1016/j.scitotenv.2016.11.193

Stuiver, M., Polach, H.A., 1977. Reporting of 14C data. Radiocarbon 19, 355–363. https://doi.org/10.1017/S0033822200003672

Sutfin, N.A., Wohl, E.E., Dwire, K.A., 2016. Banking carbon: A review of organic carbon storage and physical factors influencing retention in floodplains and riparian ecosystems. Earth Surface Processes and Landforms 41, 38-60. https://doi.org/10.1002/esp.3857.

Thomson, J., Croudace, I.W., Rothwell, R.G., 2006. A geochemical application of the ITRAX scanner to a sediment core containing eastern Mediterranean sapropel units. In: I. W. Croudace and R. G. Rothwell (eds). New Techniques in Sediment Core Analysis. London, The Geological Society of London, 65-77.

Torres, M. A., Kemeny, P. C., Lamb, M. P., Cole, T. L., Fischer, W. W., 2020. Long-term storage and age-biased export of fluvial organic carbon: field evidence from West Iceland. Geochemistry, Geophysics, Geosystems 21 (4). https://doi.org/10.1029/2019GC008632

Torres, M. A., Limaye, A. B., Ganti, V., Lamb, M. P., West, A. J., Fischer, W. W., 2017. Model predictions of long-lived storage of organic carbon in river deposits, Earth Surf. Dynamics, 5, 711–730, https://doi.org/10.5194/esurf-5-711-2017.

Turetsky, M. R., Abbott, B. W., Jones, M. C., Walter Anthony, K., Olefeldt, D., Schuur, E. A. G., Koven, C., McGuire, A. D., Grosse, G., Kuhry, P., Hugelius, G., Lawrence, D. M., Gibson, C., Sannel, A. B. K., 2019. Permafrost collapse is accelerating carbon release. Nature, 569(7754), 32–34. https://doi.org/10.1038/d41586-019-01313-4

Turner, J.N., Jones, A.F., Brewer, P.A., Macklin, M.G., Rassner, S.M., 2015. Micro-XRF Applications in Fluvial Sedimentary Environments of Britain and Ireland: Progress and Prospects. In: I. W. Croudace and R. G. Rothwell eds. Micro-XRF Studies of Sediment Cores: Applications of a non-destructive tool for the environmental sciences. Developments in Paleoenvironmental Research Vol. 17. London, The Geological Society of London, 227-265.

Vacha-Haase, T., Thompson, B., 2004. How to estimate and interpret various effect sizes. Journal of Counseling Psychology 51(4) 473-481. https://psycnet.apa.org/doi/10.1037/0022-0167.51.4.473

Vannote, R.L., Minshall, G.W., Cummins, K.W., Sedell, J. R., Cushing C. E., 1980. The river continuum concept. Canadian Journal of Fisheries and Aquatic Science 37 (1): 130-137. https://doi.org/10.1139/f80-017

von Lützow, M., Kögel-Knabner, I., Ekschmitt, K., Matzner, E., Guggenberger, G., Marschner, B., Flessa, H., 2006. Stabilization of organic matter in temperate soils: mechanisms and their relevance under different soil conditions- a review. European Journal of Soil Science 57, 426-445. https://doi.org/10.1111/j.1365-2389.2006.00809.x

Vonk, J. E., Tank, S. E., Walvoord, M. A., 2019. Integrating hydrology and biogeochemistry across frozen landscapes, Nature Communications, 10, 1–4. https://doi.org/10.1038/s41467-019-13361-5.

Warburton, J., Evans, M., 2011. Geomorphic, sedimentary, and potential palaeoenvironmental significance of peat blocks in alluvial river systems. Geomorphology 130 (3-4), 101-114. https://doi.org/10.1016/j.geomorph.2010.12.005

Wohl, E., Hall Jr, R. O., Lininger, K. B., Sutfin, N. A., Walters, D. M., 2017. Carbon dynamics of river corridors and the effects of human alterations. Ecological Monographs, 87(3), 379–409. https://doi.org/10.1002/ecm.1261.

Wolverson-Cope, F., 1976. Geology explained in the Peak District. Devon, Scarthin Books.

Yu, Z. C., 2012. Northern peatland carbon stocks and dynamics: a review. Biogeosciences, 9 (10), 4071-4085. https://doi.org/10.5194/bg-9-4071-2012

Zehetner, F., Lair, G.J., Gerzabek, M.H., 2009. Rapid carbon accretion and organic matter pool stabilization in riverine floodplain soils. Global Biogeochemical Cycles, 23 (4), 1-7. https://doi.org/10.1029/2009GB003481

**Declaration of interests**

☐The authors declare that they have no known competing financial interests or personal relationships that could have appeared to influence the work reported in this paper.

☒The authors declare the following financial interests/personal relationships which may be considered as potential competing interests:

Martin Evans reports financial support was provided by Natural Environment Research Council. If there are other authors, they declare that they have no known competing financial interests or personal relationships that could have appeared to influence the work reported in this paper.

Aged carbon mineralisation from headwater peatland floodplains in the Peak District, UK: HIGHLIGHTS

- Headwater floodplains as hotspots of old carbon turnover decline rapidly downstream
- Floodplains support microbial communities capable of respiring aged organic matter
- Lateral transfers from intact peatlands to floodplains lead to carbon emissions